THE PRODUCTION OF LOWER MOLECULAR WEIGHT HYDROCARBONS DURING THE
THERMAL DECOMPOSITION OF PULVERIZED COAL IN AIR AND NITROGEN

by

DENNIS CHARLES WEGENER

B.S., Kansas State University, 1975

A MASTER'S THESIS

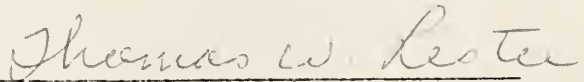submitted in partial fulfillment of the

of the requirements for the degree

MASTER OF SCIENCE

Department of Nuclear Engineering

KANSAS STATE UNIVERSITY
Manhattan, Kansas

1978

Approved by:

Major Professor

TABLE OF CONTENTS

LIST OF ILLUSTRATIONS

LIST OF TABLES

1. INTRODUCTION

1.1 Origin of the Problem

Current governmental policy, establishing coal as a primary
energy source, is based on the perceived ability of the nation's
utilities to increase substantially the use of coal without undue envir-
onmental degradation. Presently, over one half billion tons of coal
are consumed annually in the United States. More than three-fourths
of this coal is used to produce steam for electrical power generation
and other industrial requirements (1). Of the three major techniques
used in coal firing, pulverized coal, stoker, and cyclone furance
firing, pulverized coal firing is the most versatile and widely used.
Common with the other techniques, advancements in pulverized-coal firing
have primarily resulted from trial and error experimentation supple-
mented with experience and intuition. While substantial improvements
have been achieved, future benefits obtainable from this approach are
diminishing and at best are slow in coming.

Despite the vast amount of available literature concerning coal
combustion (dating back more than a century), very little is actually
known about the underlying mechanisms involved. This is due predominant-
ly to the mechanism's complexity and the associated time and money re-
quired to study it. Now, however, with the recent surge in governmental
and industrial funding and improved diagnostic capabilities, basic
research on coal combustion is being resumed. Major benefits would

accrue to society, both economically and environmentally, if the present upsurge in basic research in coal can be incorporated into the design of future pulverized coal firing units. One of the more widely studied aspects of pulverized coal combustion is its thermal decomposition or, as more commonly termed, its devolatilization. Studies commonly examine the effects of heating rate, final temperature, reaction time, particle size, pressure, and composition of the surrounding atmosphere on the devolatilization process. The ultimate goals of the studies are to determine what role this devolatilization plays in the overall combustion process and how this role may change as a function of the above parameters.

There are a multitude of problems associated with fundamental pulverized coal devolatilization research. Among the more formidable are: laboratory simulation of large scale facilities, the use of nondisturbing diagnostic equipment, and a means of obtaining meaningful gas samples. Few, if any, of the more cited experiments on coal devolatilization managed to overcome all these problems. This has resulted in the emergence and surprising acceptance of several hypothetical combustion mechanisms based almost solely on ambiguous data, obtained in such a manner as to be unrepresentative of true combustion behavior.

In an effort to circumvent certain of the more intractable experimental difficulties, the region behind the reflected shock wave of a single pulse shock tube (SPST) has been employed in the present study. With a SPST coal particles are rapidly heated to the high temperatures associated with combustion. The particles are maintained at these temp-

eratures for short, yet controllable lengths of time (hundreds of microseconds), and subsequently quenched at rapid rates. Nondisturbing optical diagnostics are readily applied to a SPST whose gas-dynamic characteristics allow a fixed-group of particles to be observed throughout the reaction sequence. Post-shock sampling of the quenched volatiles does not disturb the reaction zone as do the gas sampling probes of flat flames and furnaces.

Samples taken after shock-heating the coal were analyzed for their C_1-C_4 hydrocarbon volatile contents. The results were plotted versus temperature for coal samples heated in nitrogen (pyrolysis) and air (oxidation). By comparing these plots, a plausible combustion mechanism was formulated.

The use of the region behind the reflected shock of a SPST for coal devolatilization studies has not been heretofore attempted, and thus a major effort was required to adapt the use of the SPST to the collection of reliable data from coal suspensions. Under experimental conditions common to more established techniques, the approach of this experimentation yielded consistent results.

An extensive review of the most pertinent studies on pulverized coal devolatilization is first provided. This review is followed by a detailing of the experimental techniques, the results, proposed mechanisms, and conclusions.

1.2 Review of Literature

Comprehensive literature surveys are available which address the thermal decomposition of pulverized coals (2,3) and the hypothesized role that decomposition plays in the combustion process. These review articles list well over a hundred references which are concerned with the role played by devolatilization on the pre-ignition and early combustion behavior of many coals. A review of the majority of these studies reveals at once the difficulty in designing unambiguous experiments on coal combustion. Discrepancies in the data presented from many studies can be associated often with the varying experimental techniques employed. The articles reviewed in this section are the most germane to the analysis of the data from the present experimentation. Discussions of the articles are arranged in groups by the magnitude of their heating rates.

The familiar standard proximate or ASTM analysis is the most widely known of the methods employed in which the heating rate is relatively slow. The volatile and fixed carbon contents of the coal are determined by placing 1 gram of coal in a crucible and heating at a rate of 15°C/sec to a temperature of 950°C. The volatile content is determined by the weight loss during seven minutes at 950°C, and the remaining char, excluding the ash, is termed the fixed carbon. The standard proximate analysis technique has been used for many years as a standard means of classifying coals of various origins and types. It should be noted that the ASTM procedure only serves as a basis from which the fixed carbon and volatile yields of different coals can be compared; the yields there-

by obtained are not, however, intrinsic characteristics of the coal
which can be expected to be obtained at other heating conditions.
Numerous studies conducted at both higher heating rates and temperatures
have observed volatile yields significantly higher than predicted from
a proximate analysis. This difference between the ASTM proximate
analysis and analysis of the yield at higher heating rates and maximum
temperatures is termed the Q-factor, which will be discussed later.

Crucible or similar captive experiments have been used in basic
experimentation. For instance, Wiser et al. (4) performed pyrolytic
kinetic studies of a high-volatile bituminous coal maintained at a
relatively constant temperature. The sample was placed in an aluminum
foil pan and lowered into a vertical tube furnace which was maintained
between 400-500°C. Weight loss recordings were made at various time
increments up to 1500 minutes. Modeling required segregation of the
data into three regions, each of different reaction order and activation
energy. The difficulty with which the data were modeled along with the
fact (as pointed out by Anthony and Howard (2)) that 60% of the final
weight loss had already occurred before the initial recording was taken,
have combined to render the findings questionable.

The study of Gray, et al. (5) endeavored to explain why crucible
type experiments yielded significantly fewer volatiles than most other
methods. Experiments were performed at several heating rates to the
same maximum temperature. The results obtained were plotted as percent
weight loss versus initial weight of coal in the crucible as shown in
Fig. 1.

FIGURE 1

Percent weight loss as a function of initial weight of coal
sample in crucible (equivalent to depth) for different rates of
heating and different final temperatures. (●, dT/dt=16 °C/sec,
T=950 °C;▧ , dT/dt=20 °C/sec, T=1200 °C; ○, dT/dt=0.33 °C/sec,
T=950 °C;□, dT/dt=0.50 °C/sec, T=950 °C) (After (5)).
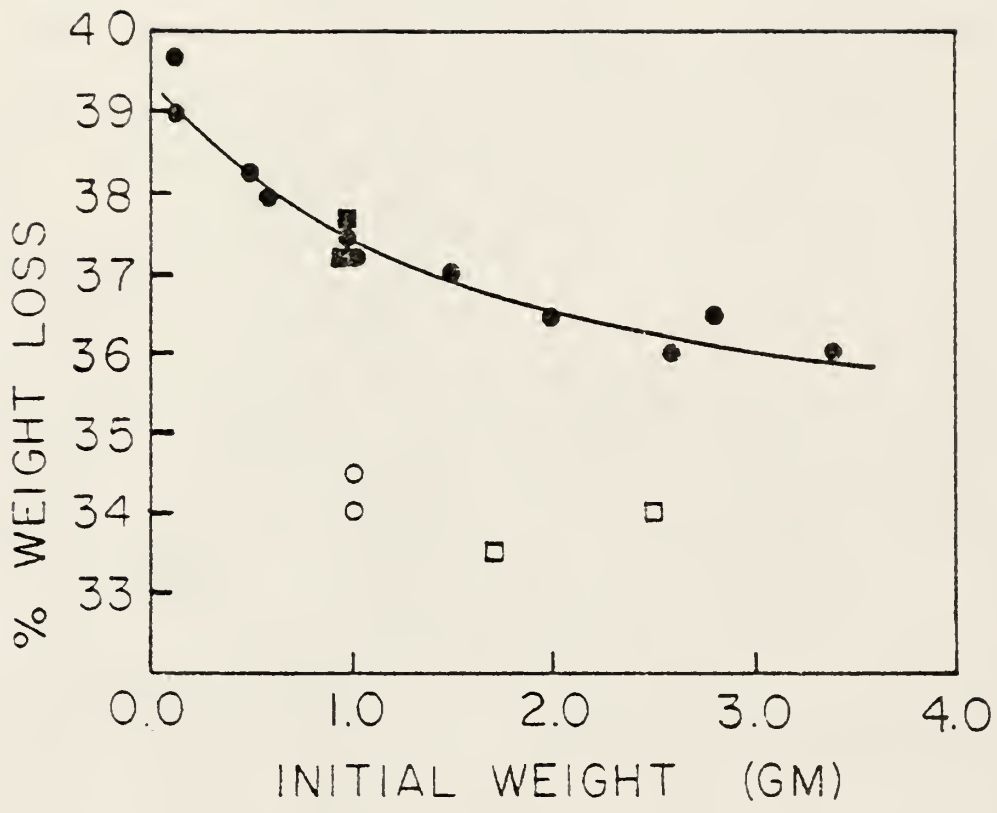
Gray et al. proposed the following two mechanisms. The first assumed that volatiles were captured while passing through the upper layers of coal. This was postulated from analysis of their data which exhibited a decrease in weight loss with coal depth. Further calculations showed, however, that this accounted for only a small percentage of the volatile yield discrepancies observed between crucible and other types of devolatilization experiments. As a consequence, a second mechanism was proposed. The authors speculated that coal was more prone to decompose when in its natural relatively unordered state. This situation was assumed to exist during rapid heat up pyrolysis in which there was no time for a restructuring of the coal to occur. Conversely, for slow heating rates, the restructuring of the coal molecule into a more orderly form was claimed to account for the decrease in devolatilization. In counterpoint, Jüngten (6), predicted that at sufficiently high heating rates negligible pyrolysis occurs during the actual heating up process. Instead, most devolatilization must be occurring at isothermal conditions. Therefore, while remaining general in their explanation, Gray et al., did manage to provide plausible explanations as to why the ASTM and other crucible decomposition studies generally yield smaller volatile contents than other techniques.

Feldkirchner and Johnson (9) enclosed coal samples in a wire mesh basket, lowered it into a preheated region, and continuously monitored the weight loss. While this was a significant improvement over the crucible studies, it still suffered many of the same limitations in-

cluding a slow heat up rate and the lack of data acquisition during the early stages in which a large portion of the devolatilization occurred.

Jüntgen and van Heek (6) looked at the volatile release from coal as a function of the heating rate. A lower range of heating rates were selected to simulate the carbonization of coal into coke. The major purposes of the study were to determine what effect higher heating rates would have on the coking process in terms of the de-volatilization, and to establish if a model, given the activation energy and pre-exponential factor, could be used to predict the temperature range of the devolatilization reactions as a function of heating rate. Two experimental methods were used depending upon the heating rates being studied. For extremely slow heating (10^{-5}°C/sec to 1°C/sec) "finely-ground" coal samples were heated at a constant rate in an electrically controlled oven. The released volatiles were carried off by helium which passed through the coal to either a gas chromatograph or mass spectrometer for analysis. At higher rates of heating (1°C/s to 10^{4}°C/sec), a few micrograms coal sample was electrically heated on a wire mesh to which a thermocouple was attached. The system was evacuated to a pressure of 10^{-4} torr. Coal particle and mesh sizings were selected such that the particles would become fixed within the mesh to achieve better heat transfer. The released volatiles were aspirated into the ion source of a time-of-flight mass spectrometer for analysis. (This procedure was not described.) In both methods (for

low and high heating rates), volatile emission rates were recorded for later conversion. Jüngten and van Heek attempted to model their results by using a set of differential equations derived in a previous publication (8). The rate of thermal decomposition was assumed to be a function of heat up rate.

Three approaches were discussed for the determination of the activation energy and the pre-exponential factor. In analyzing their data, Jüntgen and van Heek used the method they termed as "successive approximation". This method applied a regression analysis to a logarithmically reduced form of one of the differential equations (assuming first order kinetics),

$$\frac{dV}{dT} = \frac{K_o V_o}{m} \exp\left[-\frac{E}{RT} - \frac{K_o R}{mE} T^2 \exp\left(-\frac{E}{RT}\right)\right],$$

where

V = volatile release,

T = temperature,

K_o = pre-exponential factor,

V_o = maximum volatile release,

m = heating rate,

E = activation energy,

R = universal gas constant.

The authors first checked the validity of the method by showing that it could successfully model the decomposition of several simple organic compounds. However, when this author derived the logarithmic form of the differential equation, an error was found and the model is thereby questionable (see Appendix A).

There was one relevant observation that was not affected by the
error in logarithmic reduction. The authors found a marked displacement
of the major devolatilization reactions toward higher temperatures as
the heating rate was increased.

Mentser, et al. (10), at the Bureau of Mines, conducted coal
devolatilization studies at rates presumed to be comparable with those
encountered in combustion and gasification processes. Pulse-heated wire
screen cylinders were used to heat 25 mg coal samples in a reaction
chamber evacuated to 10^{-3} torr. The temperature of the wire and coal
at the end of the pulse was proportional to the duration of the current
flow. The resulting heating rate was a constant 8250°C/sec. Special
care was taken in preparing the coal samples, which were obtained by
cutting vitrains from lumps of coal. The vitrains were selected because
they provided relatively homogeneous samples which were low in ash
content. This combination was anticipated to reduce data spread. As
a final step in preparation, the vitrains were ground into particles
which fell in the 44-53 μm (diameter) size range. The devolatilization
experiments were evaluated by both weight loss determinations and mass
spectrometric analysis. Four bituminous coals of different rank and
one subbituminous coal were studied. The percent weight loss versus
temperature from this investigation are presented in Fig. 2. In all
cases studied the maximum weight loss (the plateau for the subbituminous
coal) was greater than that observed by an ASTM analysis (see Table 1).
The authors explained that the maxima in the bituminous curves were

FIGURE 2

Devolatilization of bituminous and subbituminous coals by rapid heating (approx. 10^4 °C/sec). The first four coals are bituminous and their sources are: 1b-Pocahontas No. 3, W. Va.; 2b-Lower Kittanning, Pa.; 3 b-Pittsburgh, Pa.; 4b-Colchester Illinois, No. 2, Ill. The fifth coal is subbituminous: 5sb-Rock Springs No. 7.5, Wyo. (After (10)).
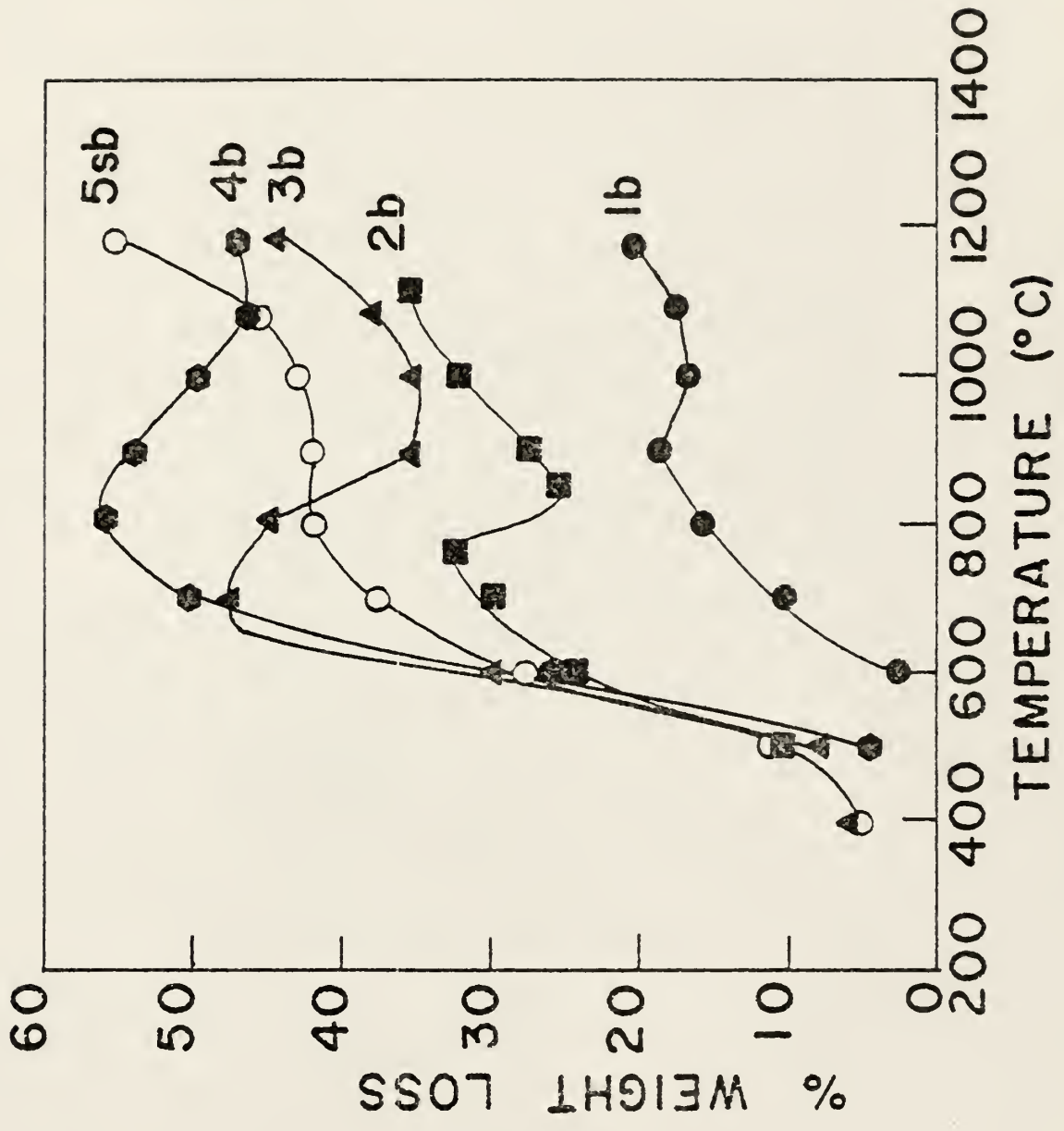
Table 1. Increased Volatiles from Rapid Pyrolysis

| Coal Source | Figure Identification | Volatile Matter Content % | | Increase Factor |
		By ASTM Analysis	From Peak Weight Loss	
Pocahontas No. 3, W. Va.	1b	16.8	18.5	1.10
Lower Kittannning, Pa.	2b	25.3	30.8	1.22
Pittsburgh, Pa.	3b	35.1	47.9	1.36
Colchester Ill. No. 2, Ill.	4b	48.0	55.8	1.16
Rock Springs, No. 7.5, Wyo.	5sb	37.7	42.4 (plateau)	1.12

the result of temperature effects on competitive decomposition and recombination reactions. No attempt was made to explain the plateau and subsequent sharp increase demonstrated by the subbituminous coal.

Mass spectrometric analyses found H_2, CH_4, and CO to be the major components of the produced gases. Of the higher molecular weight hydrocarbons observed, the authors pointed out that acetylene, a major constituent of other studies, was not present. They attributed its absence to the lower temperatures and heating rates employed in their study.

The production of tar was also monitored via weight loss determinations. (Weight loss associated with the gases was determined from the pressure increase in the reactor vessel.) The formation of tar was favored at low decomposition temperatures.

Anthony et al. (11,12) looked at the rapid devolatilization of a lignite and bituminous coal in helium and partial hydrogen environments. A technique was employed in which 10 mg coal samples of presumably mono-layer thicknesses were sandwiched between wire meshes. A two-branch, resistor-controlled heating circuit was used to regulate the heating rate and final temperature which could be varied respectively between 65 and 10,000°C/sec and 400 and 1100°C. Volatile yield was determined by weighing the sample (coal and screen) before and after heating. A particle size distribution of 53-83 μm (diameter), with a mean diameter of 70 μm (whether the mean diameter was based on number or mass was not discussed) was used for all experiments except where particle size was a

variable. In addition to varying the particle size, the effects of residence time, pressure, heating rate, hydrogen partial pressure, and final temperature on weight loss were also examined. Volatile yields (weight loss) increased with increasing temperature (to some plateau), increased with decreasing particle size, (the increase was small in helium but greater in hydrogen), and increased with decreasing pressure, except when in the presence of a hydrogen rich environment where volatile yields increased. The authors' explanation for this was based on the assumption that numerous parallel decomposition reactions were needed to describe the formation of primary volatiles and the ensuing sequence of secondary reactions leading to the formation of char. It was their contention that hydrogen, at sufficiently high partial pressures, can interrupt these secondary reactions at intermediate stages and subsequently lead to the production of more volatiles.

Examination of the temporal runs showed that most of the devolatilization occurred during heat up for even the most rapid heating rate, 10,000 °C/sec. (This does not agree with the previously discussed predictions of Jüngten (6)). Anthony et al. found only a slight dependence of volatile yield on heating rate, a finding at variance with the later conclusions of Kimber and Gray (18). Anthony et al. believe that reported increases in volatile yields with increasing heating rates may have been the result of measures taken to achieve higher heating rates and not the heating rate itself. Such measures were, the use of smaller particles, better particle dispersion, and other techniques which may have allowed the escape of reactive intermediate species prior to formation of char.

The authors reported that small, but significant, weight losses occurred during the cooling process since the mesh was cooled at approximately 300°C/sec by radiative and convective heat transfer. These additional losses were determined by an iterative computer procedure based on a kinetic model developed from the data.

The authors made no attempt to collect and analyze the volatiles. This was left as a complimentary study, which was eventually performed by Suuberg et al. (13). This study employed the same experimental apparatus and techniques as Anthony et al. (11,12); however, product composition was measured. The char and tar were determined gravi-metrically while the gas and light liquids were analyzed by gas chromato-graphy. All experiments were conducted in an inert (helium) environment.

As before (11,12), two coals were studied; a Montana lignite and a Pittsburgh bituminous. As may have been predicted, the product yields from lignite pyrolysis were dominated by oxygenated species. From their data, the authors identified five phases in the pyrolysis of lignite. Listed with increasing temperature, the five phases identified were:

1) low temperature removal of moisture < 450°C

2) low temperature CO_2 and hydrocarbon evolution 450-600°C

3) evolution of pyrolytically formed water 600-700°C

4) evolution of hydrocarbons, hydrogen, and carbon oxides 700-900°C

5) evolution of carbon oxides > 1000°C.

They went on to postulate that the low temperature CO_2 was likely a pro-duct of decarboxylation reactions, and that the evolution of pyrolytically

FIGURE 3

Yield of methane from lignite pyrolysis to different peak
temperatures.   Curve obtained from first order model. (After (13))
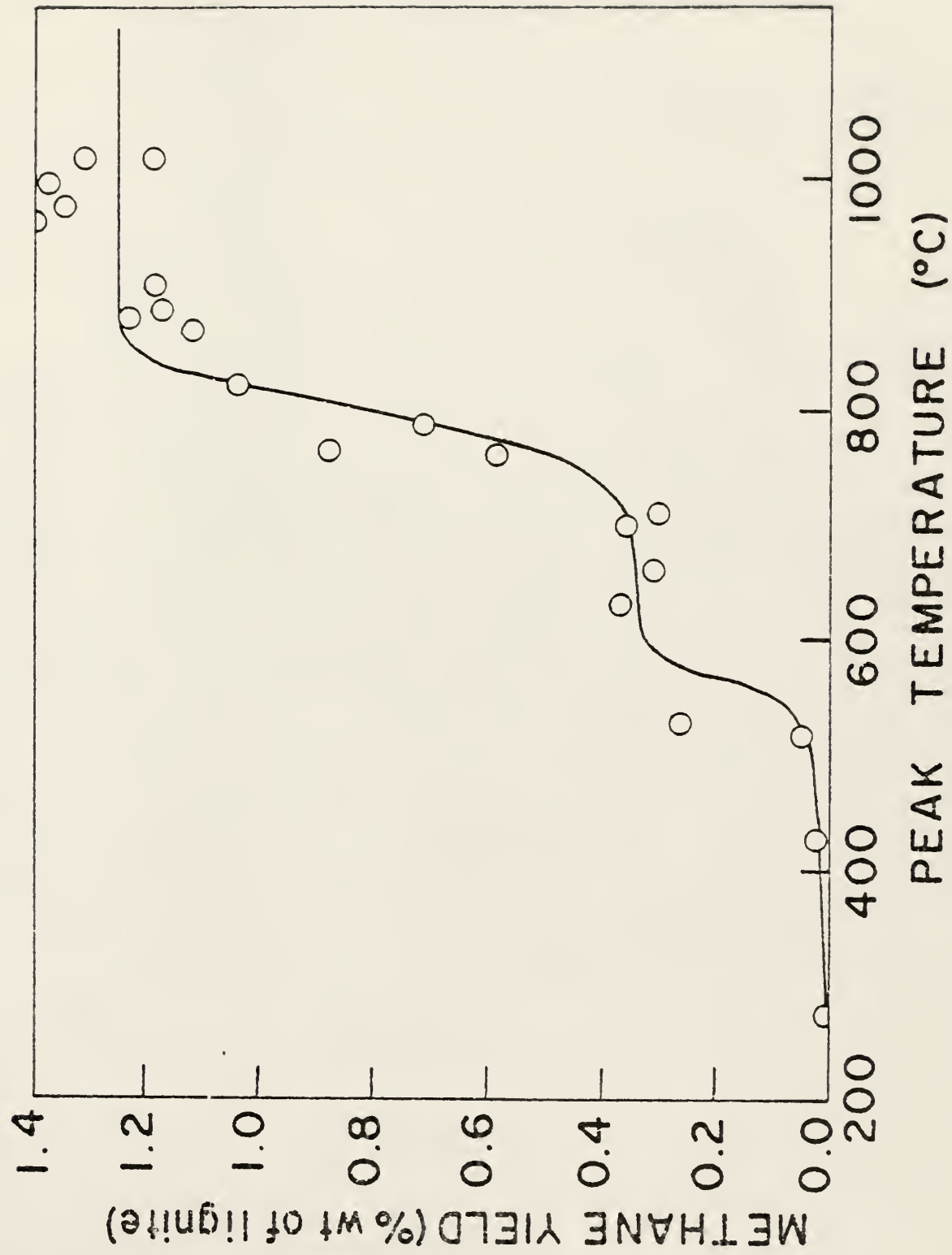
formed water resulted from phenolic decomposition. This phenolic decomposition can also be used to account for the plateau observed in the methane yields versus temperature (see Fig. 3). (Recall that a plateau was also observed with a subbituminous coal in Menster et al's. work (10)). The intermediate hydroxy groups are believed to consume hydrogen ions, otherwise available for stablization of hydrocarbon radicals. If not stabilized, these radicals are likely to recombine and form char as opposed to bonding with hydrogen and contributing to the volatile yield.

The bituminous coal yielded results strikingly different from the lignite. With this coal, the product yields were mainly hydrocarbons; the major part of which were recognized to be heavy tars (molecular weight greater than 300). The methane yield as a function of temperature is given in Fig. 4.

While it was difficult to identify specific phases (as done with the lignite), four general phases were distinguished.

1) low temperature removal of surface moisture ($< 300°C$)

2) evolution of pyrolytically formed water ($300-400°C$)

3) a broad phase involving softening of the coal, accompanied by tar and hydrocarbon evolution ($400-900°C$)

4) evolution of CO and H_2 ($> 900°C$)

The authors were not able to provide sound explanations as to why the pyrolytically formed water evolved at lower temperatures with the bituminous coal than with the lignite. They attributed the observed dissimilarities to possible differences in the chemical nature of the hydroxyl bonds.

FIGURE 4

Yield of methane from bituminous coal pyrolysis to different peak

temperatures. Curve obtained from first order model. (After (13))
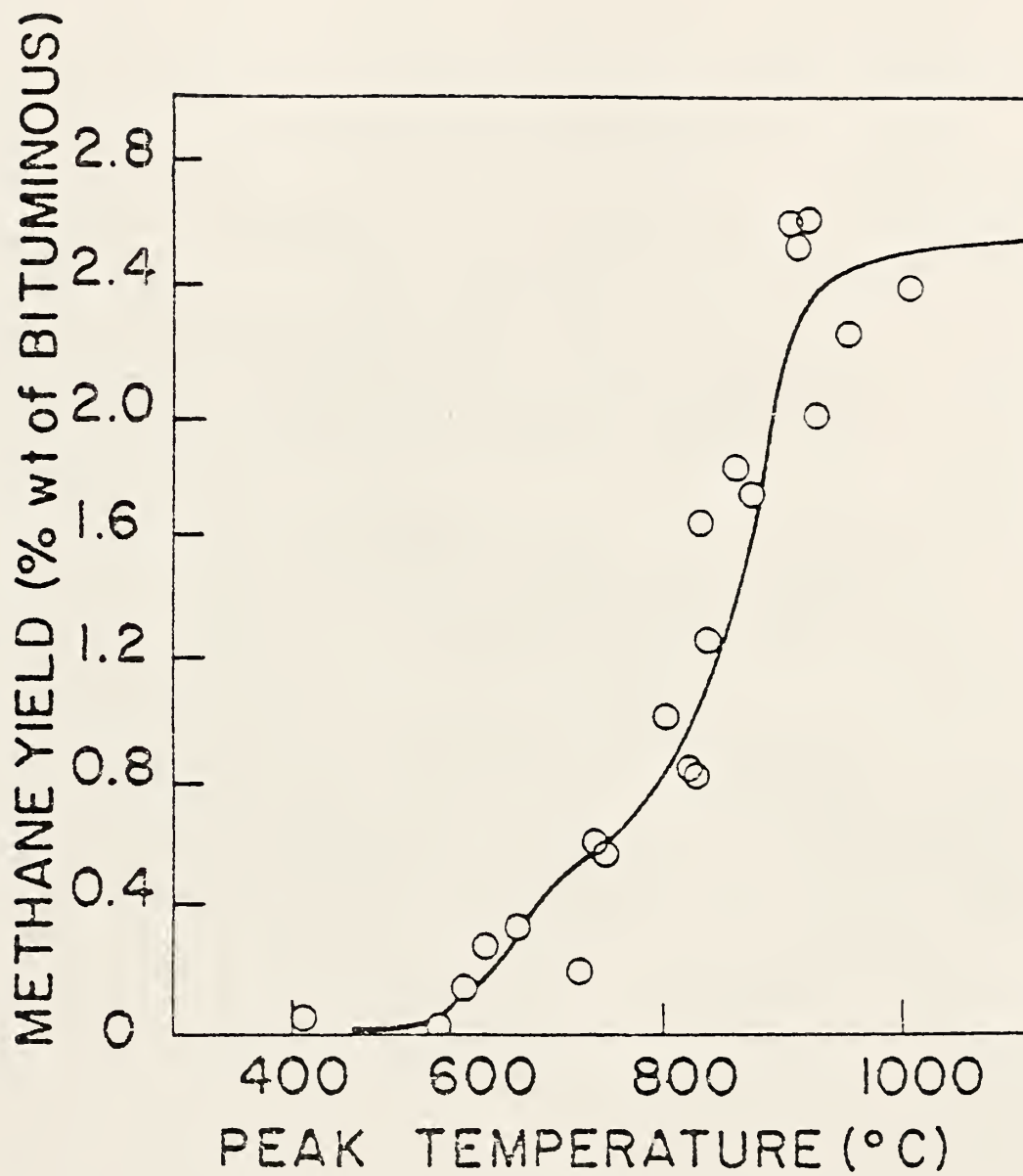
Because the oxygen content of the bituminous coal was significantly less than the lignite (8.1 wt.% as opposed to 18.2 wt. %), the absence of a methane plateau with the bituminous runs somewhat supported the reason for its existence with lignite. The lesser amounts of elemental oxygen found in bituminous coal versus lignite pointed to the presence of fewer hydroxyl groups in the parent coal molecule. The relative scarcity of hydroxyl groups permitted more of the hydrogen radicals to stabilize reactive hydrocarbons throughout the temperature range studied. This produced the observed continuous increase in the methane yield with increasing temperature for the bituminous coal as compared to the stepwise increase (believed to result from the dominance of phenolic decomposition reactions from 600-700°C) observed with the lignite coal.

In addition to the above, Suuberg, et al., also looked at the sulfur and nitrogen content of the pyrolyzed chars of the two coals. For both coals, sulfur was found to be more easily removed than nitrogen. At pyrolysis temperatures to 1000°C, 66-75% of the original nitrogen but only 33-50% of the original sulfur remained in the char.

A limited number of experiments were performed (with the lignite) which looked at the effects of helium pressure and particle size on volatile yield. From these runs, a significant decrease in total volatile yield was observed as the pressure was increased from 10^{-4} to 69 atmospheres. Similar, yet smaller, effects were also observed with increasing particle size. By further analysis of the data the reduction was found to be primarily the result of decreased tar and liquid evolution.

Conversely, the gaseous hydrocarbon and char yields, of much smaller
concentration, were found to increase with pressure. From this obser-
vance, the existence of competitive mechanisms was hypothesized. One
mechanism involved the transport of tar and liquids away from the particle,
and the other involved cracking reactions within the particle. Large
effects of pressure were not observed below 10 atm and tar cracking
reactions first became significant above 800°C (below which the tar
yield demonstrates no pressure dependence). As in the previous studies
of Anthony, et al. (12,13) little dependence on heating rate was observed.

Suuberg et al. also examined their data with respect to combustion.
By determination of the product of the surface volatile flux and the
heating value of the volatiles, the distance of a volatiles flame front,
at a given heating rate, from the center of a coal particle was calculated.
If the distance was less than or equal to the particle radius, the vola-
tiles flame front was assumed to be on the surface of the coal particle
which implied a heterogeneous ignition or combustion process. Conversely,
if the distance was greater than the particle radius, the flame front was
assumed to have moved off the particle surface. (The term critical dia-
meter represents, for a given set of conditions, the particle size at
which the flame front is just located on the particle surface.)

In analyzing their data, the authors discovered that the flame front
could not be maintained off the surface for the lignite coal until temp-
eratures exceeding that required to ignite the solid surface were obtained.
From this observation, heterogeneous ignition and combustion processes

were assumed to precede movement of the flame off the particle surface. Further calculations predicted, for a heating rate of 10^4°C/sec, that at no time would the flame front move off the surface for particles less than 55 μm in diameter.

Similar calculations performed on the bituminous coal lead to the same conclusions. The heterogeneous mechanism was shown again to precede movement of the flame off the particle surface. For the bituminous coal heated at 10^4 °C/sec, the critical diameter was calculated to be 45 μm. This is a factor of two to three larger than the critical diameters of 15 and 29 μm from the earlier studies of Howard and Essenhigh (14,15,16,17).

These earlier studies (14,15,16,17) used the one-dimensional flame of a vertical plug-flow furnace to study devolatilization and its effects upon ignition and subsequent combustion of a Pittsburgh Seam coal (generally less than 200 μm diameter). A water cooled probe was used to collect solid samples at various distances along the flame axis. These distances were eventually converted to time by consideration of the coal flow rate, the temperature profile, and the assumption of conservation of moles.

Upon collection, the solids were analyzed by a slightly revised ASTM proximate analysis technique. From initial analysis of the data, it was determined that very small amounts of devolatilization occurred prior to ignition. With ignition, the first detectable decrease in fixed carbon content was observed and a subsequent, more rapid decay of volatile matter occurred.

Because the fixed carbon content was observed to decrease just after ignition and before the volatile content began to rapidly decay, it was

decided that ignition was beginning on the particle surface (heterogeneous ignition). This conclusion, that heterogeneous combustion precedes volatile combustion, was later attacked by the Bureau of Mines. (A review of their work follows the discussion of this study.)

Howard and Essenhigh separated volatile losses into two components, one being due to gaseous evolution and the other resulting from heterogeneous combustion. Based on this assumption and the acceptance of a model which described pyrolysis to be a volumetric reaction, two equations were developed to quantitatively analyze the data. Subsequent calculations indicated that approximately seventy percent of the volatile matter loss resulted from gaseous evolution as opposed to twenty-five percent from heterogeneous combustion. The other five percent of the volatile matter remained in the solid residue.

The activation energy for the gas evolution was determined by applications of first order Arrhenius behavior to the amount of undecomposed volatile matter. Because of the dramatic change in decomposition rates at ignition, activation energy calculations were divided into two regimes. The activation energy calculated for the pre-ignition regime was 6 kcal/mole, while that for the post-ignition regime was 28 kcal/mole.

From pre-ignition volatile concentration analysis and calculations of a critical particle diameter, the authors concluded that volatile concentrations surrounding the particle were too low to support ignition. As an alternative, they reasoned that "ignition originates on the solid

surfaces of particles, and that the rate of flame propagation is independent of the rate of pyrolysis".

Kimber and Gray (18), with the British Coal Utilization Research Association (BCURA), performed devolatilization experiments on a low rank coal at heating rates of 10^5-10^6 °C/sec and final temperatures up to 2200°K. Their method involved feeding size-graded coal particles through water-cooled probes into an isothermal laminar flow furnace. Two size distributions were studied with mean diameters of 30 and 50 μm. Known weights of these particles were carried by a laminar flow of preheated argon into the reaction zone at the center of the furnace (the walls of which were also preheated). Subsequent to the time-controlled devolatilization process (18-110 msec), the particles were quenched by a water-cooled brass collector at an approximate rate of 10^5 °C/sec. The laminar flow enhanced this process by keeping the particles in a narrow beam as opposed to turbulently dispersing them. After quenching, the particles were separated from the gas by a cyclone and weighed. In some cases, a proximate analysis of the char was also performed (all coals were analyzed before testing).

The authors report the following three findings from their data: (1) devolatilization at high heating rates appears to be a two-stage process, (2) the amount of weight loss increases with increasing heating rate, and (3) the amount of weight loss increases with increasing temperature. However, what may be the most important finding of the study comes

from experiments in which proximate analysis determinations before and
after the devolatilization are available. From these determinations a
quantity termed commonly the "Q factor" can be calculated. The Q factor
is described generally as the ratio of the weight loss to the change in
volatile matter. (While often used, this is a somewhat inadequate
definition. This author finds a better understanding can be obtained
by studying Fig. 5, which is self-explanatory.)

From their calculations Kimber and Gray found Q to be greater than
one in all cases. In order for this to be true some of the ASTM fixed
carbon must be gasified in addition to the initially determined volatile
matter. This finding is of significant interest since it negates the basis
from which Howard and Essenhigh (14,15,16,17) concluded that heterogeneous
combustion takes place on the particle surface prior to observance of
ignition. Their conclusion was based on a loss of fixed carbon in the
flame front which can also be explained (as shown by Kimber and Gray
(18)) as a Q value greater than one. In other words, fixed carbon, as
determined by ASTM analysis, may be gasified under rapid heating con-
ditions.

Badzioch and Hawksley (19) appear to have used the same apparatus
in their thermal decomposition studies at BCURA. The behavior of ten
bituminous and one semianthracite coals, subjected to heating rates of
2.5 - 5.0 x 10^4 °C/sec and maximum temperatures up to 1000°C, were
examined. Both heating rate and maximum temperature were significantly
lower than the previous study by Kimber and Gray (18) and nitrogen was

FIGURE 5

Explanation of the Q-factor. (From (3))
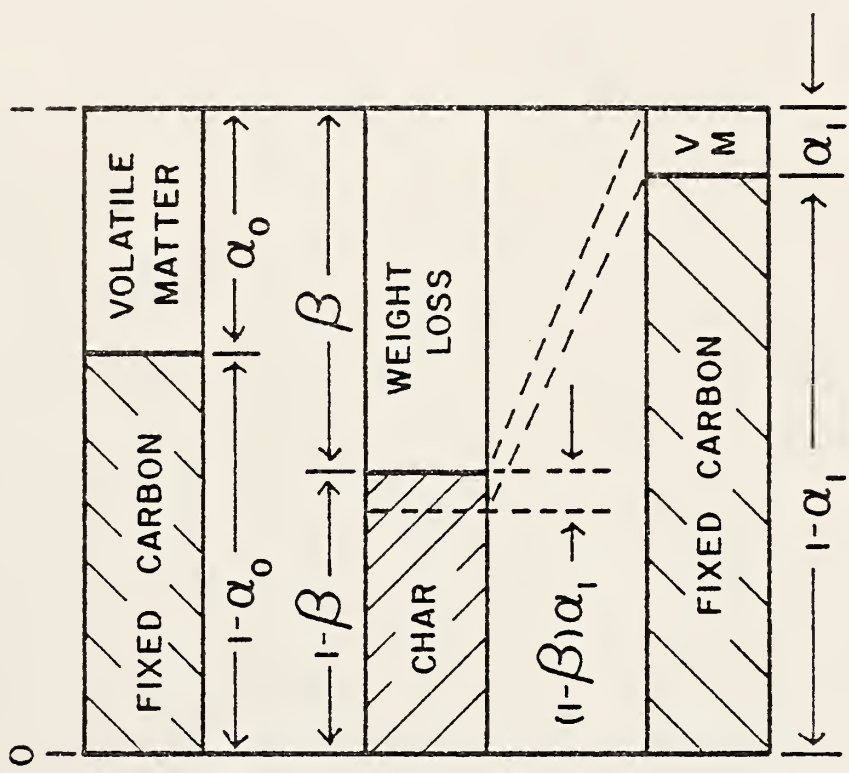
COAL $\dfrac{\text{PROXIMATE}}{\text{ANALYSIS}}$

RAPID $\dfrac{\text{HEATING}}{\text{RATE}}$

CHAR $\dfrac{\text{PROXIMATE}}{\text{ANALYSIS}}$

FIXED CARBON   VOLATILE MATTER

$1-\alpha_0$ α_0

β $1-\beta$

WEIGHT LOSS

CHAR $(1-\beta)\alpha_1$

FIXED CARBON   VM

$1-\alpha_1$ α_1

$$\text{Q FACTOR} = \frac{\text{WEIGHT LOSS}}{\text{VM}_{\text{COAL}} - \text{VM}_{\text{CHAR}}} = \frac{\beta}{\alpha_0 - (1-\beta)\alpha_1} \geq 1$$

used as the carrier gas instead of argon. This combination of lower
heating rate and lower maximum temperature resulted in a particle
agglomeration problem which was not reported in the Kimber and Gray
(18) work. Particles were found to adhere to the wall and, hence,
could not be completely recovered. In order to overcome the problem,
the authors (19) were forced to use ash as a tracer. This procedure
has several drawbacks associated with it including ash segregation and
the low ash contents of some coals studied (down to 1.1%). The authors
use of terms such as "poor reproducibility", "freak results", and
"too scattered to be reliably analyzed" to describe their data is not
conducive to its ready acceptance.

Two major objectives of the study were to develop empirical
equations for the thermal decomposition kinetics and to determine the
relationship between weight loss and the change in volatile matter (the
previously discussed Q factor). The Q factors had to be determined by a
series of indirect calculations, but did eventually agree well with the
findings of Kimber and Gray (18) (1.30 < Q < 1.95). The development of an
empirical decomposition relationship was based on isothermal decomposition
in that negligible decomposition was assumed to occur during the heating
process. (Even though this is a common assumption (6) this author,
from results of the present study, is skeptical of its applicability.)

In addition to their major concerns (19), a limited number of
experiments were conducted to study the effects of particle size and the
presence of oxygen. The results of experiments using particle distri-

butions with mean diameters of 20, 40, and 60 μm showed no significant effect of particle size. While Anthony et al. (11) did see some effect of particle size, a much wider size range of particles were studied by Kimber and Gray (18). No change in decomposition was also reported from using oxygen-nitrogen mixtures as opposed to using 100% nitrogen. However, to prevent ignition, allowable oxygen concentrations became very limited at higher temperatures (only 2% at 900°C). The degree to which these findings can be extrapolated to the higher oxygen concentrations of pulverized coal burning facilities is not clear.

In light of the observed increase in devolatilization at the expense of ASTM fixed carbon, Badzoich and Hawksley (19) (as have Kimber and Gray (18)) attacked Howard and Essenhigh's (15,16,17) heterogeneous combustion theories which are based on decreases in fixed carbon content.

Kobayashi et al. (20) conducted coal devolatilization studies at M.I.T. using a laminar flow furnace which was a modified version of the furnace used in the BCURA studies (18,19). Their experiments examined a lignite and a bituminous coal at heating rates of 10^4 - 2×10^5 °K/sec and at temperatures from 1000-2100°K. Samples of 0.1 to 0.3 g of size graded coal (38 μm - 44 μm diameter) were injected into the reaction vessel with an argon carrier gas, and following devolatilization, were quenched at rates up to 10^6 °K/sec and collected.

Volatile yields were determined in this study by two commonly used methods: weight loss and ash tracer. Of these two methods, the ash

tracer method was found to be more prone to error. The authors presented figures of weight loss versus time at six different furnace temperatures for both coals. As expected, higher volatile yields were obtained in shorter reaction times as the furnace temperature was increased. Data for the two coals were also fitted with a first order model and yielded activation energies and pre-exponential factors of 25 kcal/mole and 6.6 x 10^{-4} sec^{-1} respectively.

Ubhayakar et al. (21) studied the rapid devolatilization of a bituminous pulverized coal injected into hot combustion gases. The flow times of the coal-gas mixture through the gasifier were controllable between 7 to 70 msec. Heating rates and maximum temperatures up to 10^5 °K/sec and 2250 °K, respectively, were reported.

After devolatilizing for a selected dwell time, the particles were quenched by eight jets of cold water. The volatile yields were determined by both char and gas analysis. The char particles were partially collected in a funnel at the bottom of the gasifier. Since no attempt was made to recover all the particles, ash tracer analysis was used in lieu of the somewhat more reliable weight loss method. Gas samples were taken prior to quenching and analyzed by gas chromatography and an on-line IR detector. Little emphasis was placed on the the gas analysis which reported only H_2 and CO_x. Large discrepancies were found to exist between the two methods of analysis and considerable effort was expended to provide explanations. It was concluded that volatile cracking accounted for a significant part of the observed differences. This cracking was

found to increase with higher coal loadings and was believed to occur

partially within the particle (10-20%).

Blair et al. (22) performed a study of the compounds evolved

during the controlled pyrolysis of coal. While many of the results

are beyond the scope of this study, several of the findings are of

interest. Two methods were used to heat the three bituminous coal

samples: one termed a pyroprobe and the other a graphite ribbon.

The graphite ribbon was used solely for weight loss experiments since,

with its use, particle heating rates were not controllable. The other

device, a pyroprobe, consisted of a platinum ribbon. The ribbon was

bent into a "V" shape to hold the particles. It could be heated to a

maximum temperature of 1400 °C at controllable rates up to 2×10^4 °C/sec.

A gas chromatograph was used in conjunction with the pyroprobe to identify

and measure the evolved gases. The pyroprobe was also used in the experi-

mental determination of time resolved gas evolution rates. Measured

species concentrations included CH_4, CO, CO_2, C_2H_2, C_2H_4, C_2H_6, HCN, and

NH_3. Of interest to this study are the hydrocarbon concentrations shown

individually on a mass fraction of the coal sample basis in Fig. 6 and

cummulatively on a weight percent basis in Fig. 20. By comparing the

quantity of light gases to the total weight loss, it was determined that

much of the evolved material was not accounted for by the gas analysis.

This unaccounted weight loss was presumed to be "heavy ends" which had

boiling points in excess of 750°C and which were never eluted from the

GC columns. These heavy ends were believed to be the result of the rapid

FIGURE 6

Major species detected as fractions of coal sample
versus temperature. (After (22))
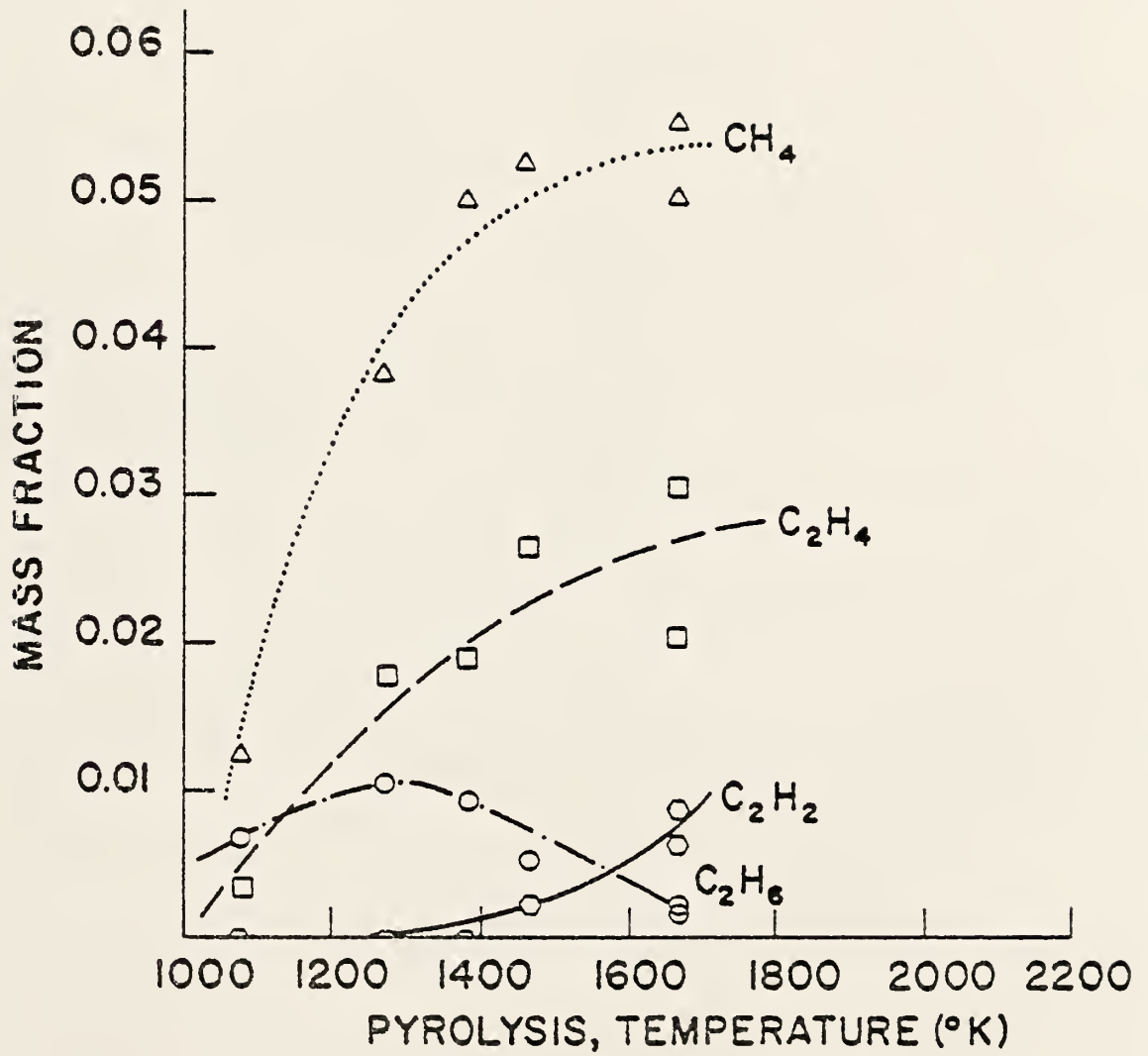
quenching experienced by volatiles upon being eluted from the particle surface.

The rate of gaseous evolution was modeled by considering the process to be a physical one (as opposed to chemical) that could be described by basic fluid flow concepts. A fitting of the model to the Wyodak coal data (the subbituminous coal), yielded a pre-exponential factor and activation energy of approximately 1.37 sec^{-1} and 2.1 kcal/mole respectively.

It is apparent thusfar that much contradictory evidence has been presented. In a recent review, Essenhigh (23) discussed the historical evolution of philosophies of the combustion behavior of coal particles. According to Essenhigh, there is wide acceptance of the following mechanisms involved in coal combustion. Large particles ($D>100\mu m$) pyrolyze and burn under diffusion control. Smaller particles pyrolyze and burn, or ignite, pyrolyze and burn. Under extreme conditions (e.g., explosion), particles may ignite and burn heterogeneously without significant occurrence of pyrolysis. The author has perhaps overstated the degree to which the last conclusion is accepted. Several groups, notably the Bureau of Mines and BCURA, are not convinced that heterogeneous ignition is important. That particles ignite in the gas phase under many conditions (especially slower heating rates and larger particle sizes) appears well founded. The particle sizes and environmental conditions under which either a heterogeneous or homogeneous mechanism predominates, however, have not been agreed upon.

Recently Goldberg and Essenhigh (24) performed coal combustion studies in a jet-stirred reactor. The authors concluded that their data were "apparently" but "not necessarily" at variance with earlier findings of Howard and Essenhigh (17) in which ignition was deduced to be both heterogeneous and prior to the major evolution of volatiles. It was hypothesized that at the higher heating rates of their study (10^6°K/sec versus 10^4°K/sec in the earlier research), heterogeneous ignition may still have taken place, but this heterogeneous process was immediately suppressed by a high volatile flux. The duration of this heterogeneous combustion was presumed to be short enough to avoid detection. The authors speculate that at even higher heating rates, it is possible that pyrolysis may be completely suppressed during the reaction. Goldberg and Essenhigh supported their assumption by a selective assessment of Nettleton and Stirling's shock tube research (25,26,27). (The heating rates of a jet-stirred reactor and shock tube are comparable.)

The most complete shock tube study of devolatilization was conducted by Woodburn et al. (28) who used a vertical tube with the driver section at the top. The coal particles (37-44 μm) were placed in suspension by a circulation blower which piped the coal particle-test gas mixture upward through the test section. Four test gases were used in their study: argon, argon + hydrogen, argon + iodine, and argon + hydrogen + iodine. The addition of hydrogen and iodine were done respectively to observe the effects of hydrogenation and an initiator. Heating rates were on the order of 10^5-10^6°K/sec.

Post-shock gas analysis to detect the evolved hydrocarbons was performed with a gas chromatograph. The results of the gas analyses for runs conducted in argon is given in Fig. 7 which shows the total hydrocarbon yields and the product distribution of these yields (based on percent weight of the reacted coal) versus temperature. The authors noted a major difference between the results of their study and other, more conventional, devolatilization studies. In most studies methane was by far the major gaseous hydrocarbon present, while in their work notable yields of unsaturated hydrocarbons (up to 50%) were discovered. The authors implied that this may be the result of a shorter reaction time.

The major problem of this study stemmed from the dispersion of coal particles throughout the test section and the use of the incident shock to heat the particles. By using this method the authors subjected the coal particles to a continuum of dwell times up to some maximum dwell time. Another shock tube study of coal devolatilization was reported by Lowenstein and von Rosenberg (29). In their study a high volatile bituminous coal (14-54 μm diameter) at low mass loadings was heated behind the reflected shock in an argon test gas to temperatures between 1000-1500°K. A pneumatic coal injector was used to disperse the coal particles just prior to bursting the diaphram. Measurements of pressure, visible light absorption, and IR emission (at several wavelengths) were obtained from oscillograms taken during the devolatilization process (behind the reflected shock). Although the

FIGURE 7

Total C_1-C_4 hydrocarbon yields, as a percent weight of
the original coal sample, versus gas temperature behind the in-
cident shock. (After (28))
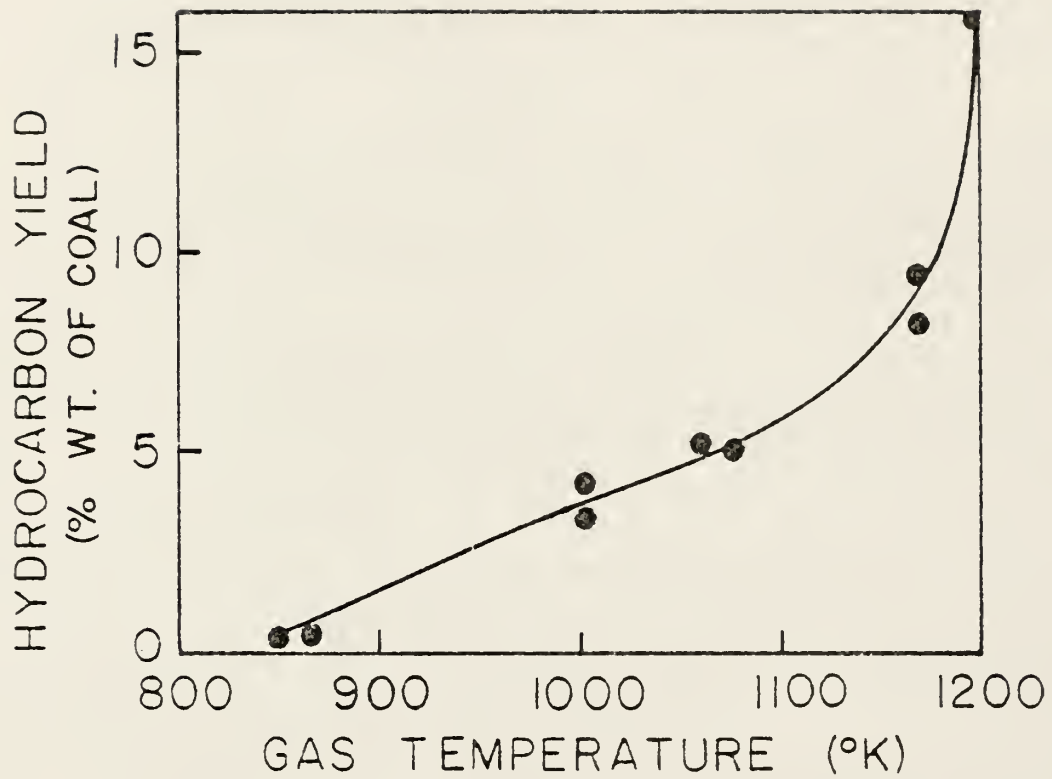
technique shows promise, no gas analysis was performed.

This completes the literature review of a number of the more notable publications on coal devolatilization. Several general conclusions which could be drawn from the review are:

1. Devolatilization yields increase with increasing maximum temperature.

2. The effects of particle size and pressures on volatile yields may be significant over extremely wide ranges but are generally found to be small in the ranges most commonly used.

3. The effect of heating rate on volatile yields is not yet established. While it is generally accepted that experiments employing the higher heating rates usually find volatile yields in excess of those predicted by an ASTM proximate analysis (Q>1), some argue the increase is not due to the higher heating rates, but is the result of procedures taken to achieve the higher heating rates.

4. Rapid heating rates tend to shift major devolatilization fluxes to higher temperatures.

5. There is disagreement as to whether the volatiles are primarily released during or after particle heat-up (especially when rapid heating rates are used).

6. Coals of lower rank (lignite and subbituminous) tend to exhibit plateaus in their devolatilization curves at intermediate temperatures.

7. The majority of the devolatilization studies have relied on weight loss and ash tracer methods to determine their devolatilization yields. Recently, however, trends toward species identification and measurement have been emphasized.

8. Whether ignition and subsequent combustion is of a heterogeneous or homogeneous nature, or even a combination of the two, is not clear. Furthermore, it is not certain under which conditions heterogeneous ignition predominates.

1.3 Objectives of this Investigation

The main objective of this study is to investigate experimentally the devolatilization of pulverized coal in both nonoxidizing and oxidizing environments. Direct measurements of volatile yields in an oxidative environment just prior to ignition have never been reported. By comparing the volatile yields versus temperature in the non-oxidizing (nitrogen) and oxidizing (air) environments, it may be possible to answer, first, whether substantial pre-ignition devolatilization occurs under rapid heat up conditions, and second, to ascertain whether heterogeneous or homogeneous ignition is occurring. Two size distributions of the same coal will be used to identify possible effects of particle size.

The devolatilization studies will be performed in a single pulse shock tube (SPST) which will also be the first use of this instrument in coal research. The SPST has been selected because the temperature history and reaction time of the coal can be controlled and recorded. Moreover, shock tube operation is amendable to the study of a wide range of reaction conditions. No major alterations of the shock tube are required.

The direct measurement of lower molecular weight hydrocarbon yields will be possible through post-shock gas analyses on a gas chromatograph. Because this will be the first use of the Kansas State University SPST, a gas sampling system and the associated procedures are to be developed.

2. EXPERIMENTAL APPARATUS

2.1 The Single Pulse Shock Tube

The shock tube used in this study was designed and constructed in its conventional form by Seeker (30).   The modification to a single pulse shock tube (as depicted in Fig. 8) was required in order to collect gas samples which had been quenched after a known and controlled heating history. A single pulse shock tube (SPST), also termed a chemical shock tube, differs from a conventional tube in that only two shock waves are allowed to process the test gas. In the tube at Kansas State University, a dump tank, attached at an oblique angle to the incident shock, is used to prevent unwanted shock wave propagation.

A test is initiated when the diaphragm is ruptured. A shock front develops in the initially low pressure test region and pro-ceeds down the tube where it strikes the end wall and is reflected. The incident shock front does not propagate into the dump tank, rather, sonic flow is established between the high pressure behind the incident shock and the initially low pressure tank. The reflected shock front propagates through the sonic flow region and into the dump tank. The reflected shock is unable to advance back through the sonic flow region and is trapped (31). This insures that the reactant gas and particle sample, located near the test section end wall, are ex-posed to a high temperature pulse of known duration. If the dump tank is not used, i.e., a conventional shock tube, repeated reflections

FIGURE 8

Single Pulse Shock Tube Diagram. (From (35))
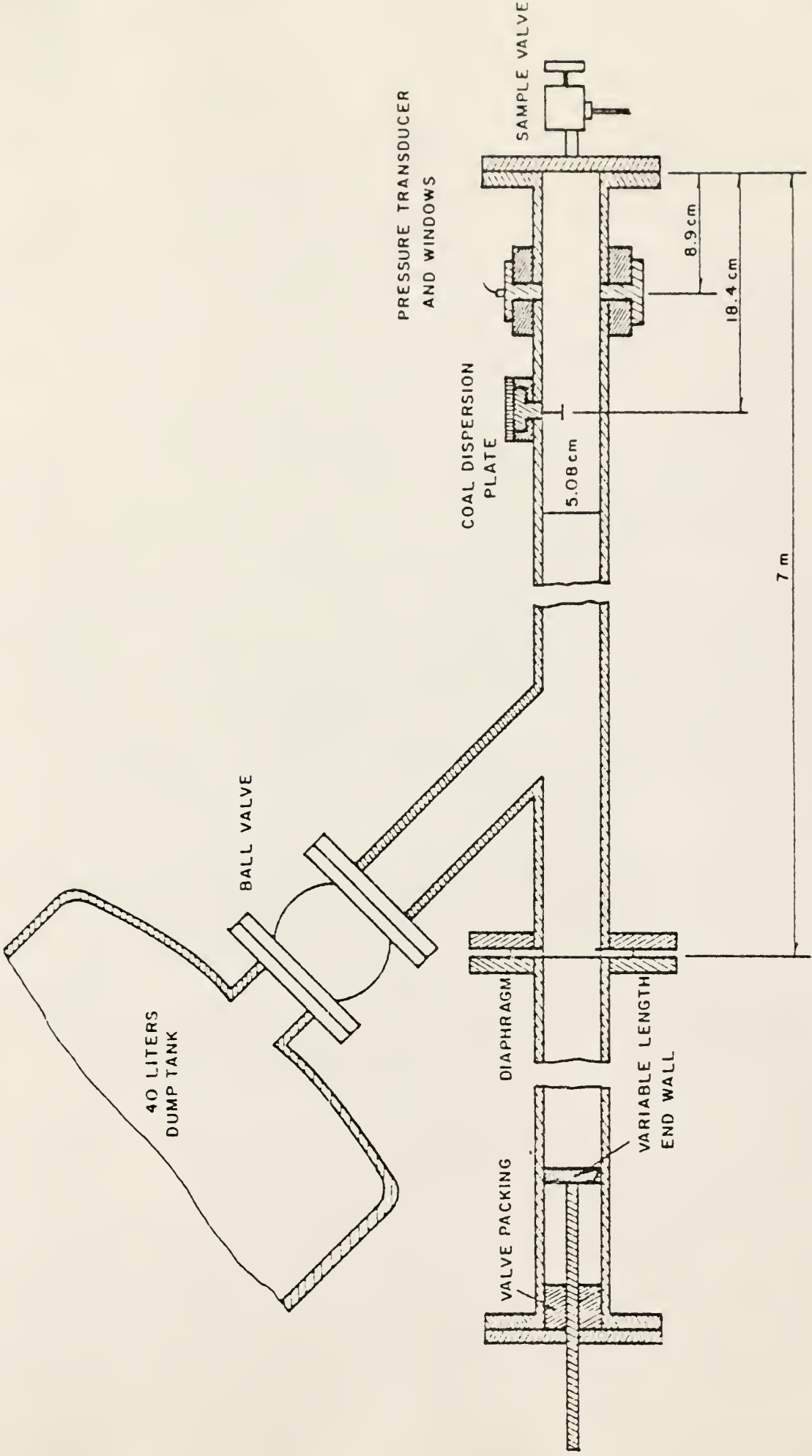
of the pressure waves subject the low pressure reactant gas and coal
to a series of temperature pulses of slowly decreasing amplitude.
The complex temperature history resulting from these pulses pre-
cludes the use of chemical analysis on the quenched gases as a use-
ful diagnostic tool.

The tube is constructed of 304 stainless steel, has an inner
diameter of 5.08 cm and a maximum overall length of 9 m. As used
in this work, the test section (or driven section) was 7 m long while
the variable length driver section was maintained at 1.85 m for all
experiments except runs in which a variable dwell time was desired.
The dump tank is stainless steel and 40 liters in volume. The volume
ratio of the shock tube to the shock tube-dump tank was .31.

Three thicknesses (3,5, and 10 mil) of mylar diaphragms were
used in various combinations to generate shocks of desired strength.
A manually operated plunger was used to burst the diaphragms, and
acceptably reproducible shocks were generated over a range of driver
gas pressures; however, superior reproducibility of the shock speed
and pressure behavior was achieved when mylar diaphragms were burst
with the plunger at over pressures comparable to their spontaneous
rupture pressure. Deviations from this practice led to varying degrees
of diaphragm opening and poor shock formation.

Helium was used as the driver gas for all runs in this study.
Test gases, nitrogen and zero air, were used for pyrolysis and

oxidation runs respectively. Gases for the study were of high purity, 99.9996% for the N_2 and 99.9998% for the zero air, and no additional purification was performed. These two test gases were ideal for comparing the devolatilization behavior of coals in oxidizing and non-oxidizing environments because they have approximately the same specific heat ratios. Consequently, equivalent initial driver and test gas pressures produced nearly the same temperatures, pressures, and dwell times behind the reflected shock wave.

Four on-line diagnostic techniques were used in this study. The speed of the incident shock was determined with two platinum thin film resistance gauges located at 38 and 59 cm from the test section end wall. Voltage pulses from these gauges were used to start and stop a time interval counter (Fluke, Model 1952B). The incident shock speed was determined by the time required for the shock to traverse the known distance between the thin film gauges.

The temperature and pressure behind the reflected shock were calculated using the frozen gas equations. The equations were derived and discussed in detail by Seeker (3) and Gaydon and Hurle (32). Twenty milligram coal samples were used for all runs in this study. At the gas pressures and temperatures used in this study, the heat capacity of the solids was only 5% of the total heat capacity of the test gas, particle suspension. The effect of the particles on the temperature and pressure of the shocked gas is not accounted for by the frozen gas equations in their basic form. Soo (33) and Kliegel (34)

suggested that proper accounting of the suspension in the frozen gas

equations can be made by incorporating the specific heat ratio of the

mixture. In the present circumstances, the alteration in the specific

heat ratio causes a change in the calculated reflected shock gas

temperature of about 50°K, still within experimental uncertainty.

The other on-line diagnostic techniques were located at the four-

port observation station, 8.9 cm from the end wall (see Fig. 9). Quartz

windows were installed in three of these ports while a Kistler pressure

transducer (Model 504A) was mounted flush to the inner wall in the fourth

port. A He-Ne laser (Metrologic) beam was passed vertically through two

of the quartz windows and detected by an RCA 931B photomultiplier tube.

The extinction of this beam was a measure of particle suspension behavior

during the experimental run. A series of apertures and mylar diffusing

screens were placed in front of the photomultiplier tube to decrease the in-

tensity of the continuum emission from the incandescent coal particles and the

laser. This emission was, however, monitored by a second photomultiplier tube

(RCA 1P28) through the remaining quartz window. The lens and aperture

configuration, shown in Fig 9, was used to focus the emission on the

photocathode of the photomultiplier tube. Temperature measurements of

the particle suspension could be deduced from emission measurements

following a technique developed by Seeker (35). All measurements were

photographically recorded from a Tektronix 551 dual beam oscilloscope.

Typical oscillograms, the details of which will be discussed later, are

given in Fig. 13. All other details of construction of the shock tube

FIGURE 9

A cross-sectional view of the diagnostics at the four-port
observation station where: A-aperture, L-lens, IF-interference
filter, M-mylar screen (reduces intensity), and PMT-photomultiplier
tube.
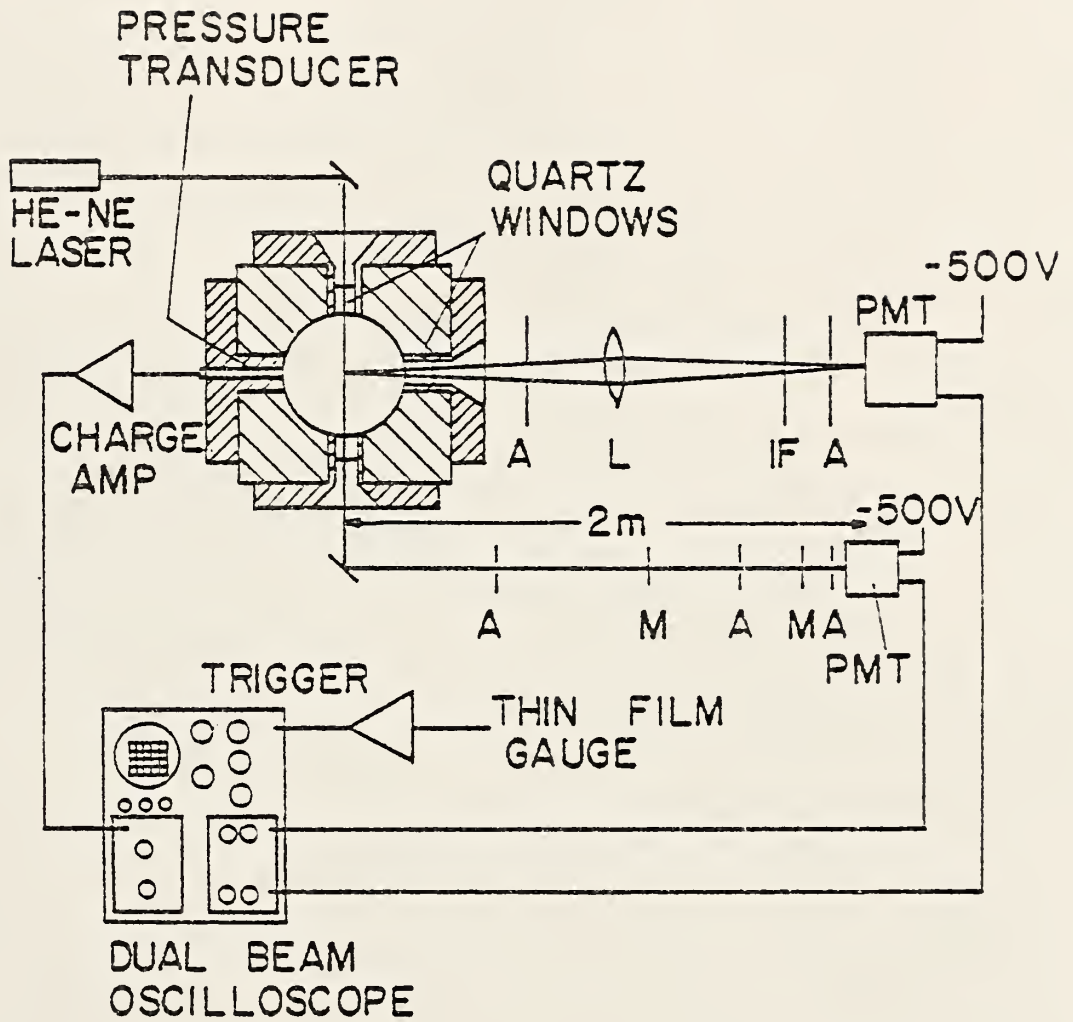
have been covered by Seeker (30). Specifics of the optical techniques have been addressed by Seeker (35) and Seeker et al. (36).

Two bituminous coals were used in this study, an Illinois No. 6 and two size distributions of a Pittsburgh seam coal. The Pittsburgh seam coals had mass mean diameters, as determined from Coulter Counter Analysis, of 13 and 25 µm and they will hence be denoted by "small" and "large" respectively. The Illinois No. 6 coal was sized by sieving through a 200 mesh standard (size of Illinois not known) screen which allowed passage of particles up to 74 µm in diameter. Size histograms of the two Pittsburgh seam coals, of primary interest in this study, are given in Fig. 10 (35).

Devolatilization of the coals was studied behind the reflected shock wave. Use of the reflected shock allowed higher temperatures to be obtained without using extremely high driver section pressures. In addition, the particle suspension was nearly stagnant after passage of the reflected shock; therefore, a fixed group of particles were observed throughout the reaction sequence, and the uncertainty in dwell time of the particles at elevated temperatures and pressures was minimized.

The coal samples were inserted into the tube on a small plate (approximately 1.5 cm in diameter) suspended from the top of the tube and located 18 cm from the end wall (see Fig. 11). The incident shock wave was used to disperse the coal particles into a fluidized cloud

FIGURE 10

Histograms of the two Pittsburgh Seam coals determined
from Coulter Counter Analyses. (After (35))
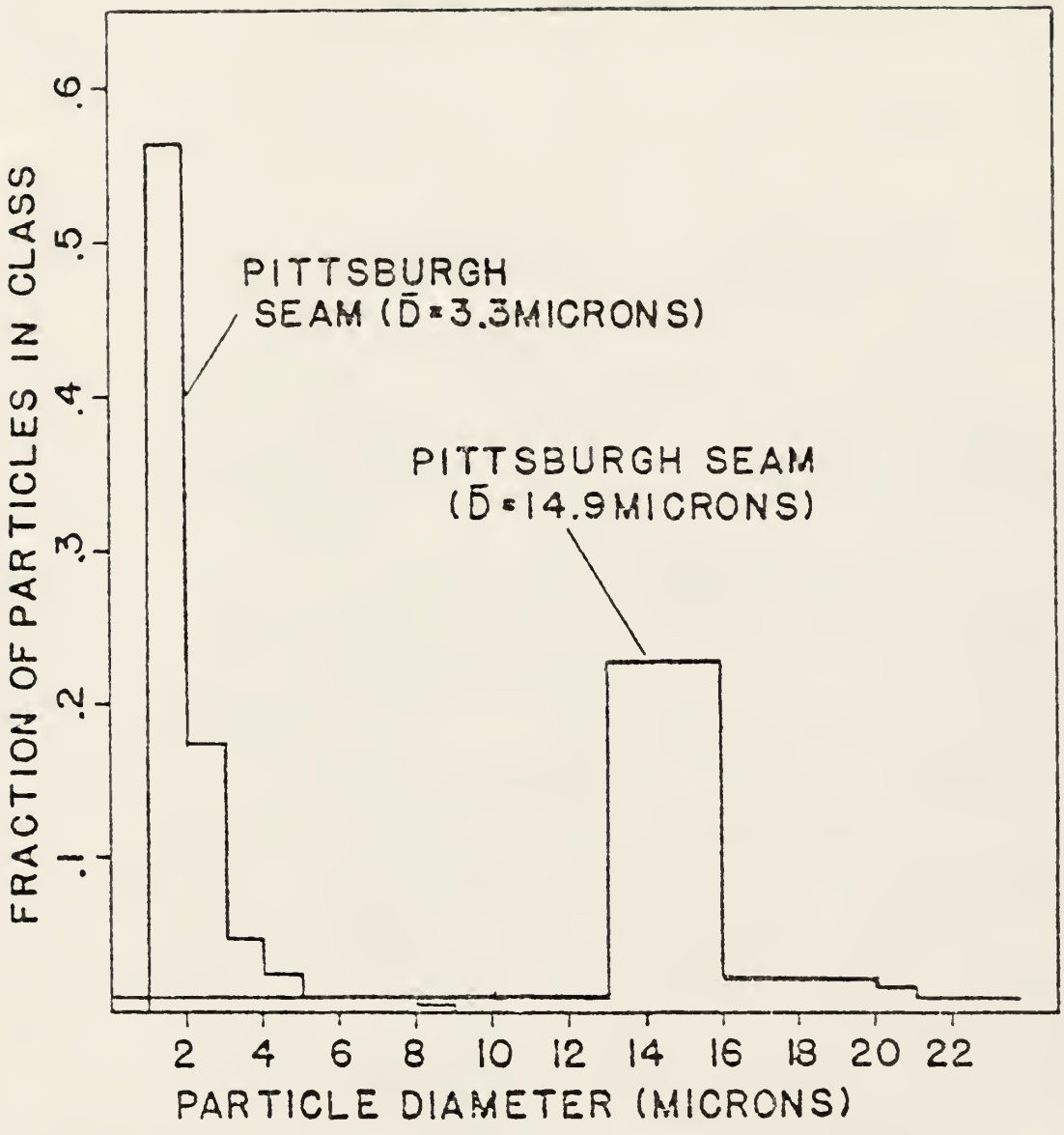
flowing toward the observation station. Subsequent arrival of the
reflected shock dispersed the cloud further, and brought it to approxi-
mately a stagnant condition over a 10 to 15 cm axial length. This be-
havior is depicted in the abbreviated X-t diagram of Fig. 11. The experi-
mental runs from which these data were obtained were performed by
Seeker (35). From optical observations of the suspension behavior
and pressure histories, Seeker et al. (35) have concluded that the
dispersion characteristics of this technique compare favorably with the
aspiration technique of Park and Appleton (37), the melenex packet
technique of Nettleton and Stirling (25,26,27) and the solenoid driver
coal injector of Lowenstein and von Rosenberg (29).

A distance-time (X-t) diagram representative of the wave systems
encountered in this study is shown in Fig. 12-a. While these diagrams
do not account for non-ideal phenomena such as shock curvature, boundary
layer effects, and incomplete opening of the diaphragms, they are use-
ful in obtaining an appreciation of the physical processes within the
tube. For instance, the temporal behavior of the suspension at a given
location, such as the observation station, can be estimated.

Of most importance with respect to the particle cloud are the
behavior of the contact surface and the incident and reflected rare-
faction head. The contact surface travels in the same direction, but
at a slower velocity, than the incident shock. Ideally it represents
the plane of contact between the driver and test gases, and the end of
the high temperature zone, region 2 (see Fig. 12-b). The reflected

FIGURE 11

Temporal behavior of particulate cloud in the shock tube reaction zone. Cloud dispersion characteristics behind the incident shock were determined experimentally (35)).

POSITION OF COAL INTRODUCTION

CLOUD MAXIMUM DENSITY

OBSERVATION WINDOW

CLOUD TAIL

CLOUD FRONT

REFLECTED SHOCK

INCIDENT SHOCK

TIME (ms)

1·0

0·5

0

DISTANCE FROM END WALL (cm)

20   15   10   5   0

DISPERSION PLATE

QUARTZ WINDOW
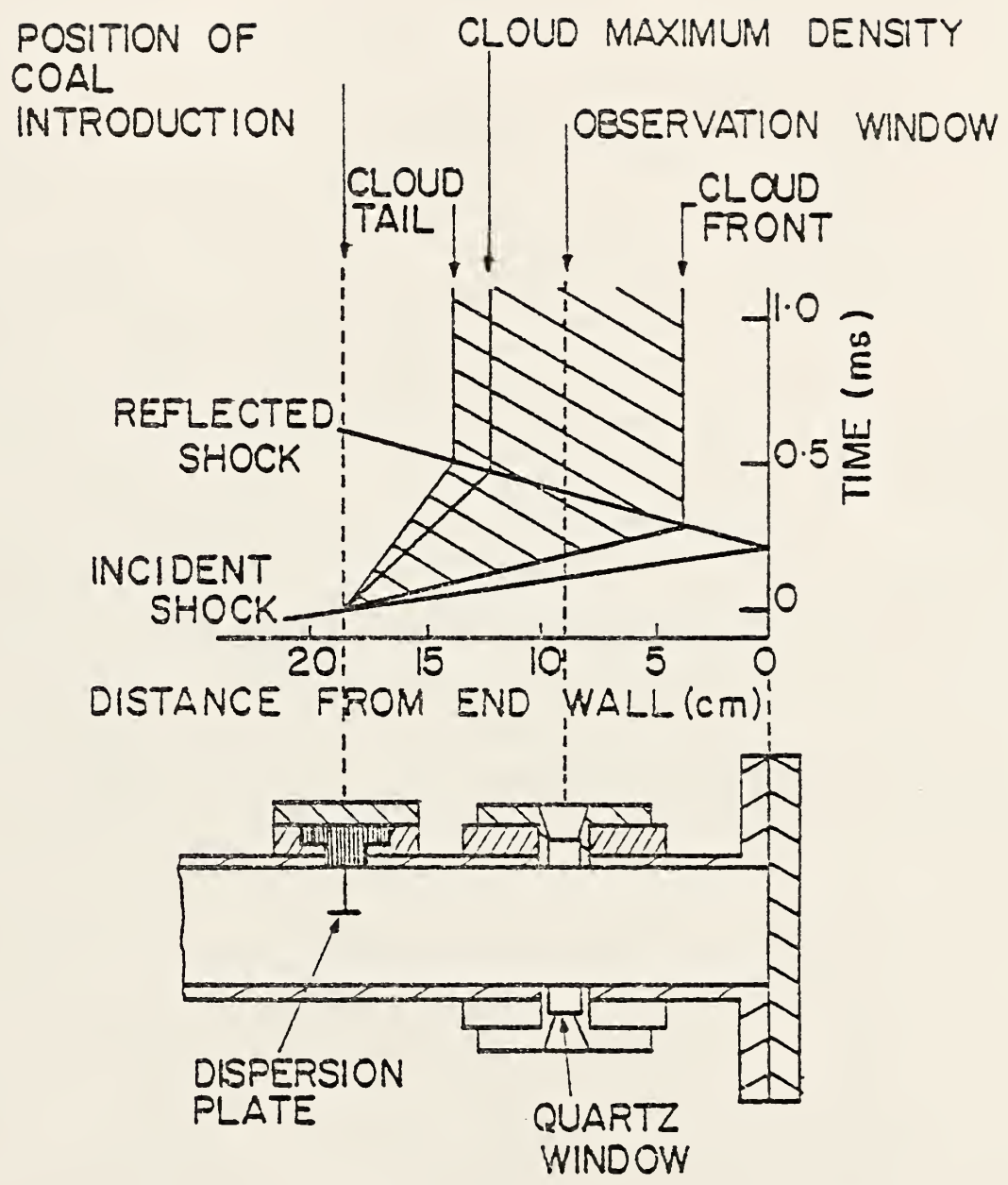
FIGURE 12

A)   An X-t diagram showing progress of the incident shock (IS),

the reflected shock (RS), the rarefaction wave (RW), and the contact

surface (CS) which separates the driver and test gases. The various

regions associated with shock tube wave diagrams are also distinguished.

This wave diagram is incomplete in that it only shows the wave inter-

actions from the diaphragm to the test section end wall.

B)   The temperature distribution at time t_1.
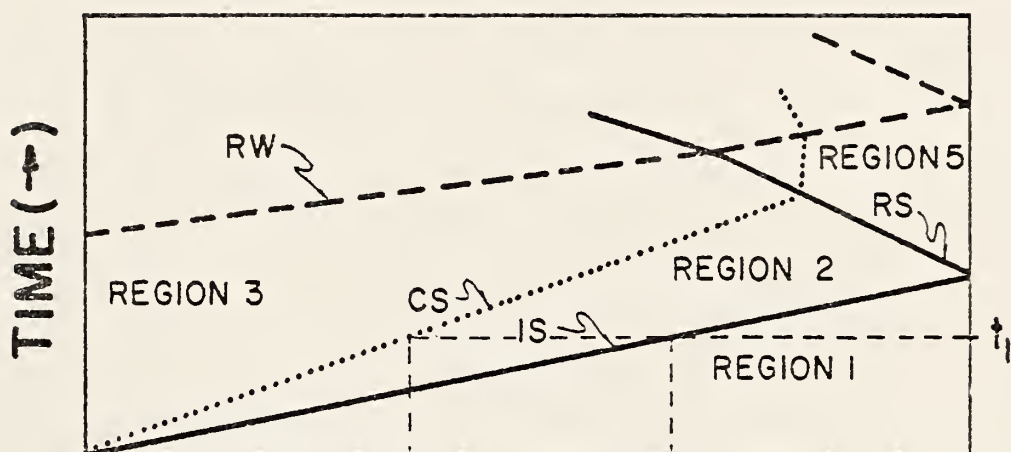
A)
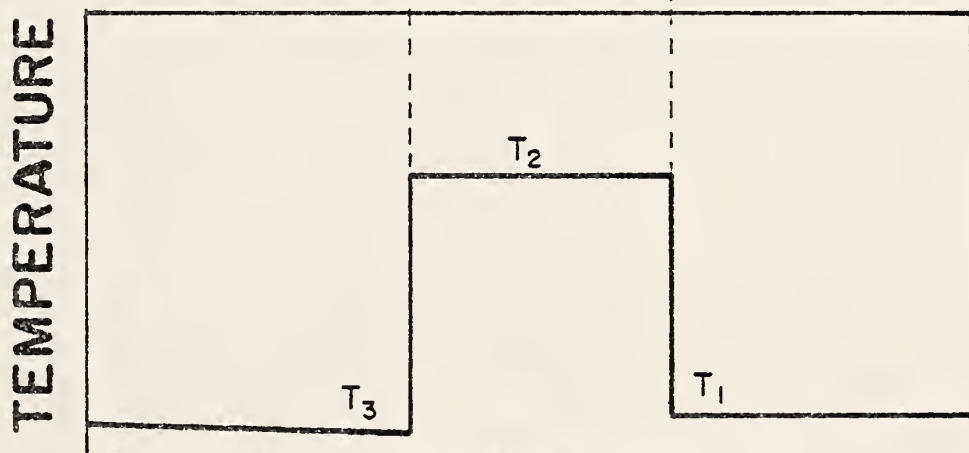
B) DISTANCE

rarefaction head accelerates through the rarefaction fan until it reaches region 3 (see Fig. 12-a) where it propagates at a nearly constant velocity, v_3+a_3, where v_3 is the velocity of the gas in region 3 relative to the tube and a_3 is the local speed of sound. Because the speed of the rarefaction head is greater at a_3+v_3 than that of the contact surface traveling at v_3, the reflected rarefaction head can be made, if the test section length is properly proportioned to the driver length, to overtake the contact surface on its propagation down the tube. This prevents excessive mixing of the hot test gas/ particle suspension with the cold driver gas and results in a rapid decay or quenching of the test suspension. In this study, except for the temporal runs, the driver section length was made sufficiently long to delay the reflected rarefaction head arrival at the observation station for approximately 1,200 μsec after passage of the reflected shock wave. This quenching occurs through an isentropic expansion which cools the hot gases at rates in excess of 10^5°K/sec.

In this study, the term "dwell time" was defined as the time interval at the observation station between passage of the reflected shock and quenching by the rarefaction wave. When the temporal runs were performed, this time was varied by changing the length of the driver section with a variable length end wall plunger. In this manner, the initiation of quenching could be varied to achieve the desired dwell time.

Non-ideal wave behavior and boundary layer influences were observed for some reflected shock temperatures and pressures. The pressure rise in Fig. 13 is basically isentropic and is common to all shock tube experimentation. It is caused by the unavoidable mismatch of accoustic impedances of the gases in regions 2 and 3. These considerations are discussed in more detail in Gaydon and Hurle (32). The influence of this temperature and pressure rise on the devolatilization kinetics is uncertain; however, since the devolatilization process is believed to be a strong function of the maximum temperature to which the coal is exposed, it was decided to express all devolatilization data as a function of the maximum gas temperature reached during the dwell time, as opposed to the initial reflected shock temperature which was determined via ideal shock relations. Insofar as the pressure disturbances are small behind the reflected shock, the resulting behavior can be modelled by an isentropic pressure-temperature relationship of the form:

$$T_5' = T_5 \left(\frac{P_5'}{P_5}\right)^{\frac{\gamma-1}{\gamma}}$$

where the primes indicate the maximum temperature and pressure and γ the ratio of the test gas specific heats.

The lengthy and detailed procedure used to prepare the shock tube for a devolatilization run was necessary to assure reproducible and reliable data. The comprehensive list of steps followed are tabulated in Appendix B.

FIGURE 13

Typical oscillograms showing pressure, laser extinction, and line emission for (A) oxidation and (B) pyrolysis of pulverized coal. (IS-incident shock, RS-reflected shock, RW-rarefaction wave; calculated reflected shock conditions; (A) 1500 °K, 6.7 atm, (B) 1400 °K, 7.1 atm; coal-Illinois No. 6).

64

(A) AIR

(B) NITROGEN
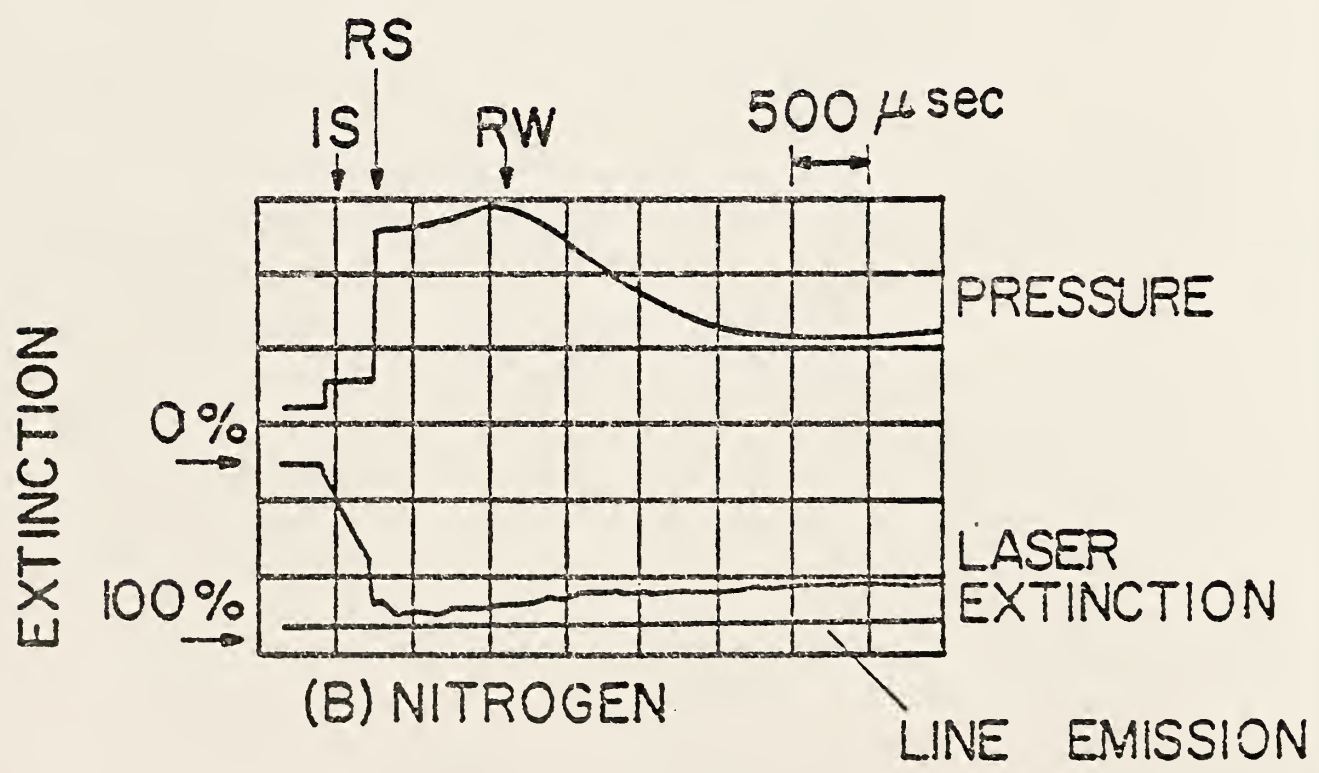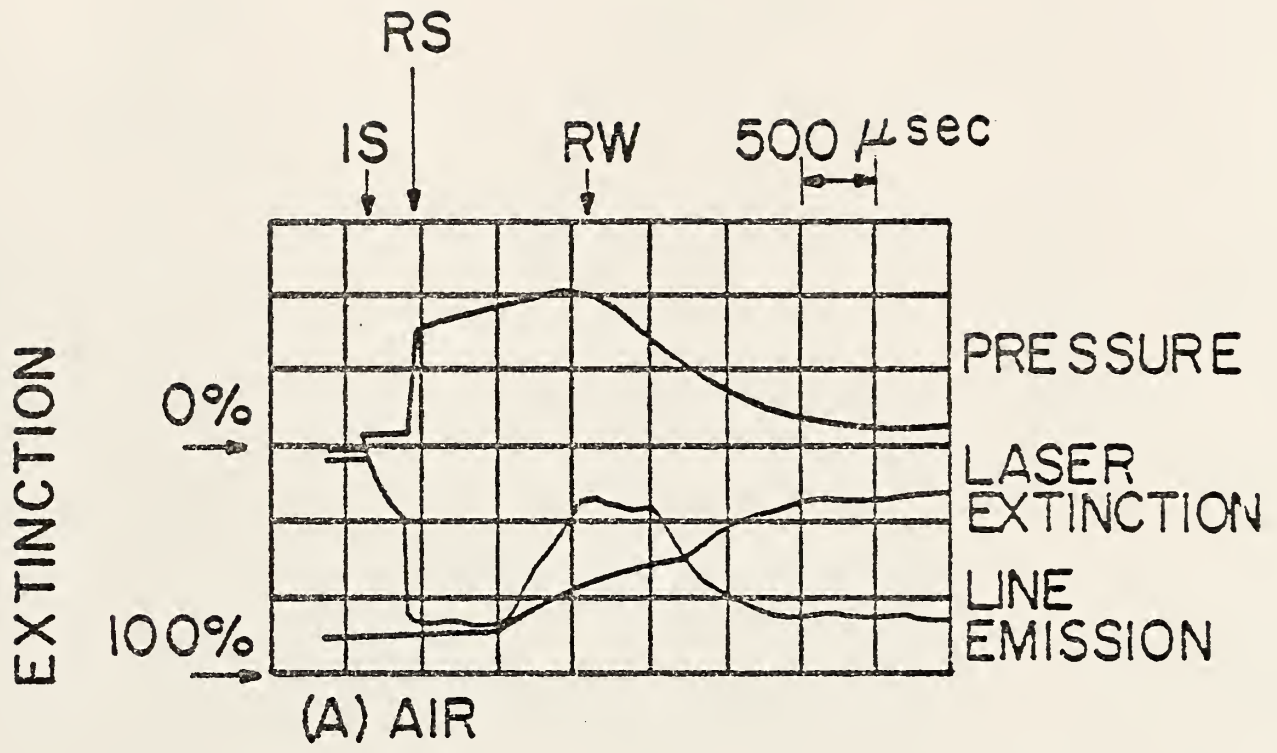
2.2 Gas Chromatographic Analysis

After the test suspension was quenched, gas samples were obtained and analyzed by gas chromatography. The gas sampling system, shown in Fig. 14, was connected to the test section end wall by a 3-way valve which was used to isolate the sampling system from the tube before and during runs, to vent the tube to a laboratory hood, or to route the test gases into the evacuated sample bottle. The 500 cm^3, stainless steel Whitney sample bottles were attached to the test section end wall with stainless steel tubing and swagelock connections. The gas was required to pass through a 7 μm filter (Swagelock-stainless steel) on its route to the sample bottle. This filter prevented the remaining larger particles from reaching the bottle and eventually contaminating the columns of the gas chromatograph.

Gas chromatographic analysis was performed on two different systems. One, a Varian 90-P gas chromatograph equipped with 6' x 1/8" molecular sieve column and a thermal conductivity detector, was used to determine the extent of driver gas mixing with the test gas. The degree of mixing, quantified by the use of a "sample dilution multiplication factor", or SDMF, was determined by matching the response of the N_2 peak from a 200 μl injection of sampled gas with the response of the N_2 peak obtained from an injection of pure test gas (either N_2 or zero air). Because the driver gas of the shock tube and the carrier gas of the chromatograph were both helium, and because the volatile concentrations were extremely low, the ratio of the injection volumes yielding

FIGURE 14

Gas Sampling System

TO VENTILATION HOOD

3 WAY
VALVE

7-μm
FILTER

TEST SECTION
END WALL

1/4" STAINLESS STEEL TUBING

VALVES

VACUUM PUMP
(WELCH-MODEL 1400)

SAMPLE BOTTLE
(500cc)

PRESSURE
GAUGE

(KINNEY-MODEL
XTG1)
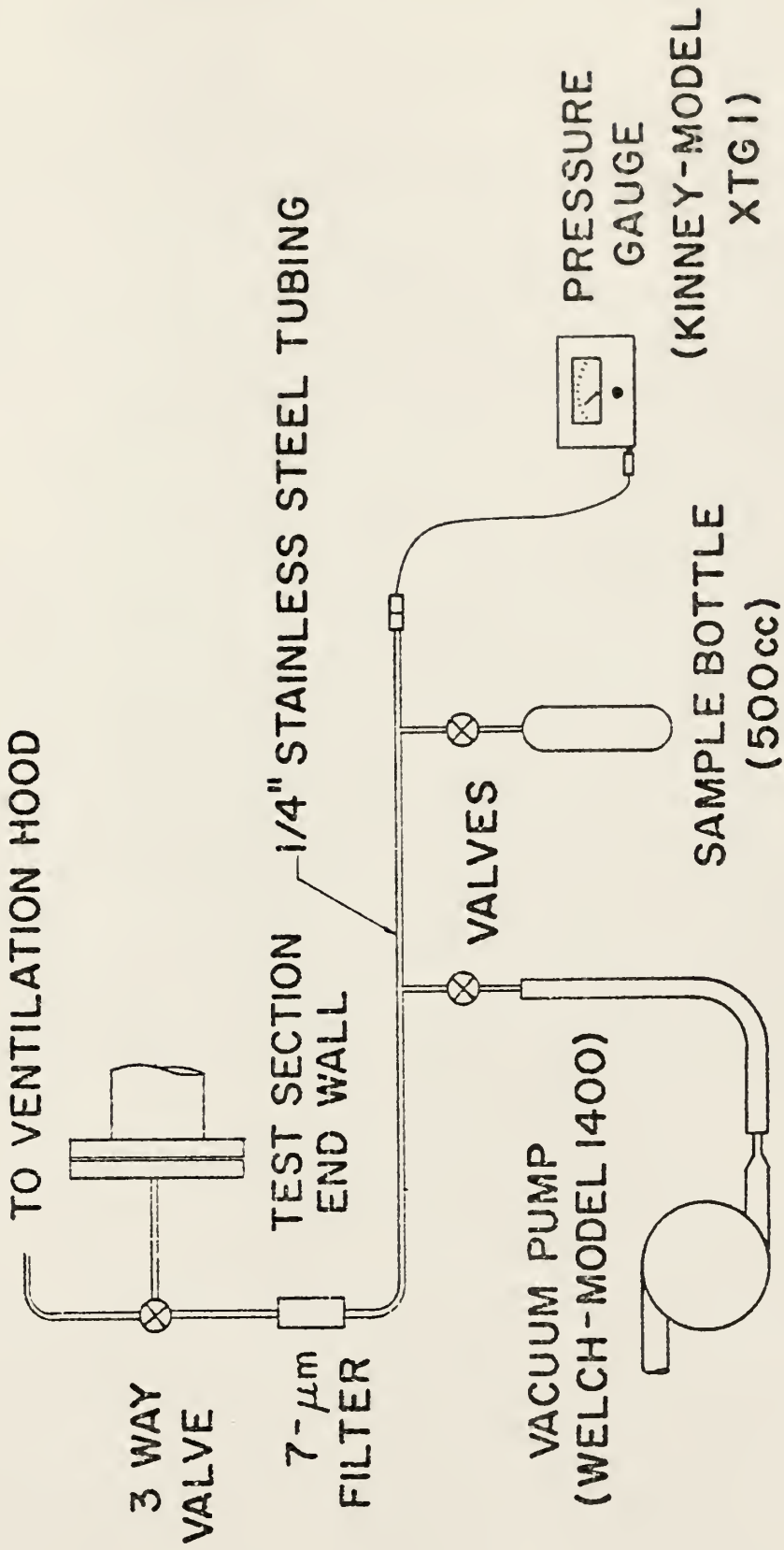
equivalent responses was directly relatable to the degree of mixing. The equation used to determine the SDMF is:

$$SDMF = \frac{200}{\delta}$$

where δ represents the volume of test gas injection needed to duplicate a 200 µl sample injection of N_2. Most values of the SDMF were between 1 (no mixing) and 3 with the larger values being associated with the more pronounced mixing of the faster shocks. While this technique was developed independently, a similar technique was used in an aliphatic hydrocarbon study by Glick (38), who included the inert tracer gas neon in his test gas.

Initially, all gas analysis was planned on the Varian 90-P, thermal conductivity gas chromatograph mentioned above. A series column configuration (a silica gel followed by a molecular sieve) was assembled to separate what were anticipated to be the major decomposition components, CO_2, CO, CH_4, C_2H_4, C_2H_6, and C_3H_8. Unfortunately, the Varian 90-P was not temperature programmable; nor did its design make it amendable to the series column configuration. These shortcomings led to separation problems which, despite the use of longer columns and different operating conditions, were never fully overcome. In addition to the separation problems, the thermal conductivity detector was not sensitive enough to detect the concentrations of the volatile products present. Consequently, this gas chromatograph was used only to determine the SDMF.

The actual analysis of test gas samples for decomposition components was performed on the second gas chromatographic system, a Tracor 550 gas chromatograph with flame ionization detector. While this detector was far more sensitive (approximately 100 times) than the thermal conductivity detector, it was not capable of ionizing CO_2 and CO, and hence it could not identify these molecules. This was unfortunate since both CO_2 and CO are known to be major devolatilization products. The flame ionization detector was, however, capable of detecting all the uncondensed, light hydrocarbons. The gas chromatograph's normal operating parameters are given in Table 2. The unsaturated C_2 hydrocarbons, C_2H_2 and C_2H_4, were not separable at the operating conditions. They were, however, separable by adjustment of several of the parameters also shown.

The gas chromatograph system was calibrated for all the above hydrocarbons. One of these calibration gases, methane, was utilized throughout the experiments to record daily fluctuations in detector efficiency.

The detector response was proportional to the number of moles and hence the concentration of the hydrocarbons. Data presented in terms of concentration, however, are not meaningful since they are specific to the experimental apparatus in which the sample is taken. Therefore, it is more desirable to express the detected hydrocarbons in terms of a more reproducible quantity such as moles of gas per gram of coal reacted or as a percent of the initial weight of the coal sample.

Table 2. Gas Chromatograph Operating Conditions

Parameters	Normal Operation	Operation
Column Packing	Porpack Q	Porpack Q
Carrier Gas	N_2	N_2
Flow rate; carrier gas	30ml/min.	12ml/min.
Flow rate H_2	400ml/min.	400ml/min.
Flow rate O_2	0.85 SCFH	0.85 SCFH
FID Temperature	130°C	130°C
Inlet Temperature	110°C	110°C
Recorder Speed	2 in./min.	1 in./min.
Programmed	yes	no, isothermal
initial temp.	50°C	30°C
final temp.	125°C	
prog. rate	25°C/min.	
initial hold	2 min.	
final hold	10 min.	

NOTE: The units correspond to those used with the instruments

This value was ascertained by assuming that the volatiles were evenly distributed throughout the test gas in which they were evolved. However, since the test gas pressure, P_1, was one of the parameters varied in obtaining different shock strengths, the number of moles of test gas present was not a constant. Hence, comparisons of concentrations between runs at different pressures is not a valid comparison of total gases evolved. These concentrations were normalized with use of the ideal gas law. The total number of moles of test gas present was:

$$n_{TG} = \frac{P_1 V_{TS}}{R \, T_{AMB}} \, ,$$

where

V_{TS} = Volume of the test section = 14200 cm^3

R = Universal gas constant = 82.05 $\frac{atm \, cm^3}{mole \, °K}$,

T_{AMB} = Ambient gas temperature ≅ 298°K

Substitution of the appropriate numerical values and the appropriate hydrocarbon concentration leads to the following formula for the number of moles of a given hydrocarbon,

$$n_{HC} = 7.64 \times 10^{-4} \, P_1 \, C,$$

where

P_1 = initial pressure of the test section (torr),

C = concentration of the detected hydrocarbon (ppm).

The mass of the hydrocarbon gas as a percent of the initial coal mass is consequently represented by

$$HC_{\%wt} = \frac{100 \ M}{W} \ n_{HC} \ ,$$

where

> M = the molecular weight of the hydrocarbon of interest,
>
> W = the weight of the coal sample = 20 mg.

This concludes a discussion of the experimental procedures used in this devolatilization study. The results obtained from their application are presented and discussed in the following sections.

3.   EXPERIMENTAL RESULTS

3.1 Devolatilization Data

Devolatilization experiments were performed with all three coals
(Illinois No. 6, Pittsburgh Seam - small, and Pittsburgh Seam - large)
in a nitrogen test gas, and with the small and large Pittsburgh Seam
coals with air as a test gas. The C_1-C_4 hydrocarbon yields were
measured after every run. These yields were converted to a percent mass
(of the total sample) basis and expressed as a function of the maximum
gas temperature. The results from experiments on the small and large
Pittsburgh coals indicated possible influences of particle size on the
devolatilization and combustion processes.

The hydrocarbon yields versus maximum gas temperatures for 44 of the
experimental runs are given in Tables 3 through 7. The temperature to
which the coal samples were heated was varied from approximately 1100°K to
2200°K. Since it was anticipated that reaction dwell time and pressure
would be important parameters, both were maintained to within ± 150μsec,
and in most cases, ± 1 atm respectively. However, even at pressures
slightly outside this range, little effect on hydrocarbon yields was
observed. To test the influence of reaction dwell time on the hydrocarbon
gas yields, a series of experiments were performed in which the dwell
time was varied from approximately 75 to 640 μsec. The yields from
these runs are given in Table 8 and shown in Fig. 15. Attempts were
made to make the runs isothermal; however variations in the driver
section length, in addition to changing the reaction time, did have

Table 3. Hydrocarbon Yields from the Pyrolysis of Illinois No. 6 Coal in Nitrogen.

Run	T_5' (°K)	CH_4 (% wt)	C_2H_2 (% wt)	C_2H_4 (% wt)	C_2H_6 (% wt)	C_3H_6 (% wt)	C_3H_8 (% wt)	$i\text{-}C_4H_{10}$ (% wt)	Total C1-C4 (% wt)
1	1209	0.05	0.00	0.18	0.02	0.13	0.00	0.17	0.55
2	1269	0.11	0.01	0.27	0.09	0.15	0.00	0.20	0.83
3	1417	0.75	0.12	1.04	0.39	0.42	0.13	0.49	3.34
4	1437	0.83	0.13	1.04	0.44	0.42	0.13	0.52	3.51
5	1483	0.85	0.17	1.02	0.42	0.36	0.17	0.46	3.45
6	1605	1.61	0.51	1.86	0.90	0.44	0.31	0.58	6.21
7	1694	2.06	0.86	2.24	0.60	0.42	0.33	0.52	7.03
8	1752	1.82	0.82	2.04	0.48	0.38	0.31	0.58	6.43
9	1812	2.60	1.61	2.81	0.26	0.27	0.42	0.41	8.38
10	1951	2.20	1.98	1.89	0.11	0.19	0.29	0.29	6.95
11	2140	1.51	3.74	1.88	0.00	0.08	0.13	0.12	7.46

Test pressures were, in most cases, maintained to within $\pm$ 1 atm and reaction times were within $\pm$ 150 μsec. Values are expressed in terms of yield of each gas as a percentage of initial coal weight.

Table 4. Hydrocarbon Yields from the Pyrolysis of Pittsburgh Seam (small) Coal in Nitrogen.

Run	T_5' (°K)	CH_4 (% wt)	C_2H_2 (% wt)	C_2H_4 (% wt)	C_2H_6 (% wt)	C_3H_6 (% wt)	C_3H_8 (% wt)	$i-C_4H_{10}$ (% wt)	Total C1-C4 (% wt)
12	1130	0.06	0.00	0.15	0.00	0.00	0.00	0.00	0.21
13	1316	0.44	0.04	0.53	0.24	0.29	0.00	0.35	1.87
14	1403	0.82	0.12	1.11	0.53	0.44	0.00	0.58	3.60
15	1528	2.05	0.44	2.25	1.01	0.84	0.13	0.99	7.71
16	1624	2.14	0.66	2.28	0.77	0.50	0.26	0.73	7.34
17	1793	4.15	2.08	3.65	0.57	0.46	0.42	0.58	11.91
18	2085	3.78	4.77	2.84	0.15	0.19	0.37	0.26	12.35

Test pressures were, in most cases, maintained to within $\pm$ 1 atm and reaction times were within $\pm$ 150 μsec. Values are expressed in terms of yield of each gas as a percentage of initial coal weight.

Table 5. Hydrocarbon Yield from the Oxidation of Pittsburgh Seam (small) coal in Zero Air.

Run	T_5' (°K)	CH_4 (% wt)	C_2H_2 (% wt)	C_2H_4 (% wt)	C_2H_6 (% wt)	C_3H_6 (% wt)	C_3H_8 (% wt)	$i\text{-}C_4H_{10}$ (% wt)	Total C1-C4 (% wt)
19	1198	0.21	0.01	0.36	0.06	0.25	0.00	0.23	1.12
20	1389	1.12	0.14	1.42	0.29	0.40	0.09	0.26	3.72
21	1397	1.12	0.16	1.48	0.20	0.44	0.11	0.20	3.71
22	1436	0.77	0.11	0.84	0.00	0.13	0.00	0.00	1.85
23	1453	0.04	0.02	0.14	0.00	0.00	0.00	0.49	0.69
24	1574	0.00	0.02	0.06	0.00	0.00	0.00	0.00	0.08
25	1695	0.00	0.00	0.00	0.00	0.00	0.00	0.00	0.00

Test pressures were, in most cases, maintained to within $\pm$ 1 atm and reaction times were within $\pm$ 150 μsec. Values are expressed in terms of yield of each gas as a percentage of initial coal weight.

Table 6. Hydrocarbon Yield from the Pyrolysis of Pittsburgh Seam (large) Coal in Nitrogen.

Run	T_5' (°K)	CH_4 (% wt)	C_2H_2 (% wt)	C_2H_4 (% wt)	C_2H_6 (% wt)	C_3H_6 (% wt)	C_3H_8 (% wt)	$i-C_4H_{10}$ (% wt)	Total C1–C4 (% wt)
26	1262	0.19	0.01	0.34	0.12	0.23	0.00	0.23	1.12
27	1421	0.32	0.05	0.42	0.15	0.17	0.00	0.17	1.28
28	1431	0.36	0.07	0.49	0.23	0.27	0.00	0.44	1.86
29	1500	1.46	0.29	1.69	0.86	0.61	0.13	0.87	5.91
30	1755	2.80	1.47	3.05	0.56	0.40	0.42	0.55	9.25
31	2033	3.99	4.11	2.88	0.14	0.17	0.31	0.26	11.86

Test pressures were, in most cases, maintained to within $\pm$ 1 atm and reaction times were within $\pm$ 150 µsec. Values are expressed in terms of yield of each gas as a percentage of initial coal weight.

Table 7. Hydrocarbon Yield from the Oxidation of Pittsburgh Seam (large) Coal in Zero Air.

Run	T_5' (°K)	CH_4 (% wt)	C_2H_2 (% wt)	C_2H_4 (% wt)	C_2H_6 (% wt)	C_3H_6 (% wt)	C_3H_8 (% wt)	$i-C_4H_{10}$ (% wt)	Total C1-C4 (% wt)
32	1161	0.00	0.00	0.10	0.00	0.00	0.00	0.00	0.00
33	1180	0.02	0.00	0.11	0.00	0.00	0.09	0.00	0.22
34	1238	0.02	0.00	0.08	0.00	0.00	0.00	0.00	0.10
35	1257	0.06	0.01	0.22	0.00	0.13	0.00	0.00	0.42
36	1436	0.31	0.07	0.61	0.03	0.15	0.00	0.17	1.34
37	1440	0.48	0.07	0.59	0.06	0.17	0.00	0.17	1.54
38	1475	0.51	0.07	0.49	0.09	0.00	0.00	0.17	1.33
39	1526	0.55	0.10	0.61	0.06	0.15	0.00	0.00	1.47
40	1545	0.46	0.10	0.48	0.00	0.13	0.00	0.35	1.52
41	1554	0.17	0.04	0.22	0.00	0.00	0.00	0.26	0.69
42	1665	0.02	0.03	0.07	0.00	0.00	0.00	0.00	0.12
43	1742	0.01	0.00	0.00	0.00	0.00	0.00	0.00	0.01
44	1801	0.00	0.00	0.00	0.00	0.00	0.00	0.00	0.00

Test pressures were, in most cases, maintained to within $\pm$ 1 atm and reaction times were within $\pm$ 150 μsec. Values are expressed in terms of yields of each gas as a percentage of initial coal weight.

Table 8. Hydrocarbon Yields from the Pyrolyses of Pittsburgh Seam
          (small) Coal in Nitrogen.

Run	T_5' (°K)	Reaction Time (µsec)	Total C_1-C_4 H. C. Yield (% wt)
45	1632	75 ± 35	3.83
46	1618	135 ± 65	3.61
47	1606	240 ± 90	5.27
48	1642	335 ± 55	4.29
49	1589	640 ± 60	8.50

Test pressures were, in most cases, maintained to within ± 1 atm and
reaction times were varied. Values are expressed in terms of yield
of each gas as a percentage of initial coal weight.

FIGURE 15

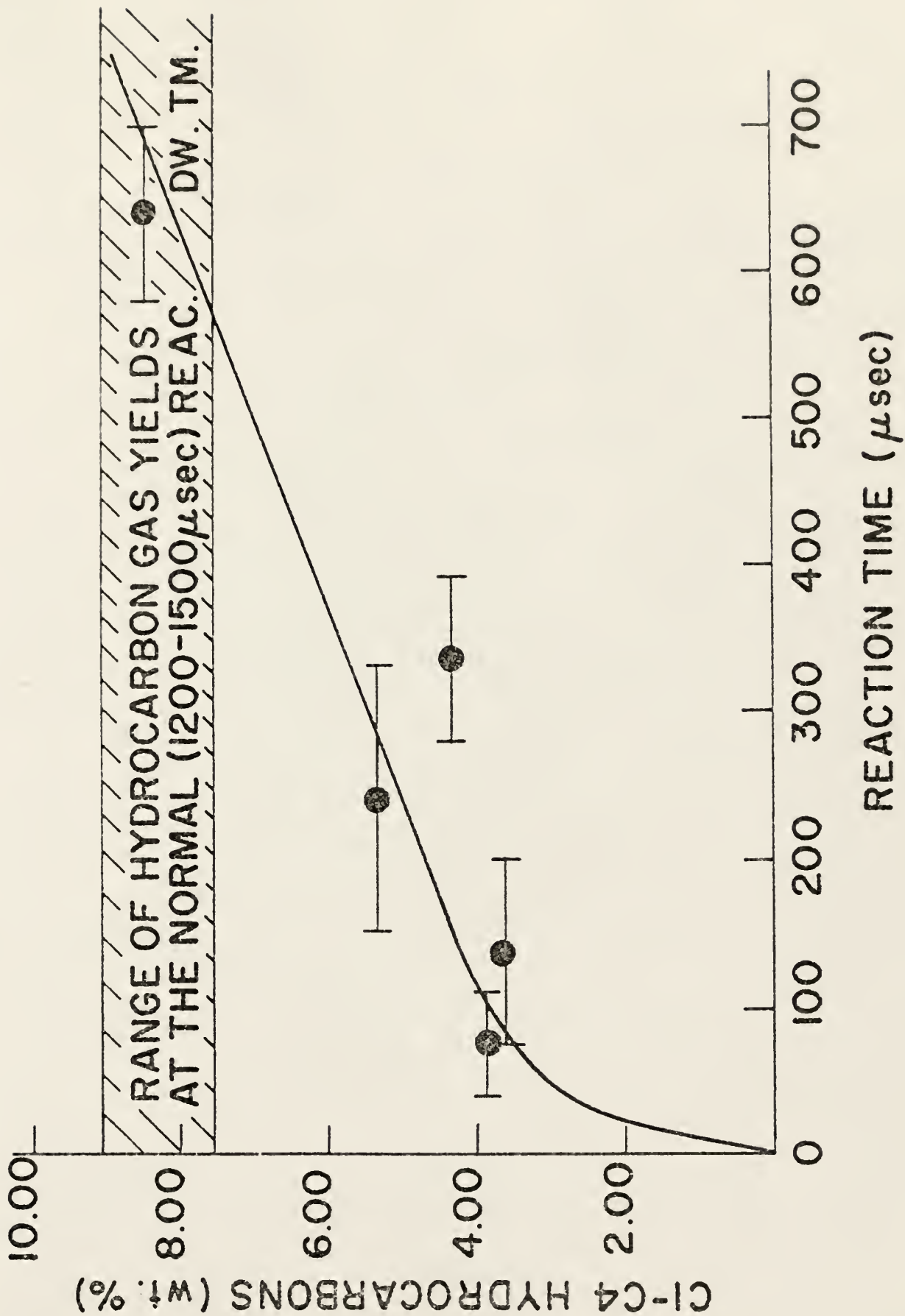Evolution of hydrocarbon gases as a function of time. Temperatures were between 1589 °K and 1642 °K; coal-Pittsburgh Seam (small).

RANGE OF HYDROCARBON GAS YIELDS
AT THE NORMAL (1200-1500μsec) REAC. DW. TM.

REACTION TIME (μsec)

Cl-C4 HYDROCARBONS (wt. %)

minor effects on the shocks' strength which made their reproducibility
with respect to temperature a problem. As a recourse, runs which fell
within the temperature range of 1589-1642°K were used to approximate an
isothermal environment. It is apparent from Fig. 15 that the hydro-
carbon evolution proceeded very rapidly, and that the variation in reaction
time between, 1,200 and 1,500 μsec should not have had a significant
effect on hydrocarbon yields. Over the range of pressures and dwell times
encountered here, it has, therefore, been assumed that gas evolution was
only a function of temperature.

Post shock analysis of the test gas following a devolatilization
experiment indicated the presence of seven low molecular weight hydro-
carbons: CH_4, C_2H_2, C_2H_4, C_2H_6, C_3H_6, C_3H_8, and C_4H_{10}. Typical gas chro-
matograms for devolatization runs in nitrogen at maximum gas temperatures
of 1250°K, 1500°K, and 2100°K are given in Fig. 16. The chromatogram
peaks are representative of the relative concentrations of the individual
hydrocarbons for all three of the bituminous coals tested. While an increase
in the integrated area under the chromatogram peaks, and consequently the hydro-
carbon yield, with increasing temperature is shown in the chromatograms, inter-
chromatogram comparisons of the magnitude of the recorder response of a partic-
ular hydrocarbon (peak) at the three temperatures should be avoided. Such a
comparison requires consideration of the sample dilution multiplication
factor as discussed previously in Chapter 2. Particularly trouble-
some in the gas analyses was the separation of ethyne (C_2H_2) and ethene

FIGURE 16

Typical gas chromatograms showing the retention times and relative magnitudes of the hydrocarbon yields at reflected shock temperatures of (A) 1250 °K, (B) 1500 °K, and (C) 2100 °K; coal-Pittsburgh Seam (small).
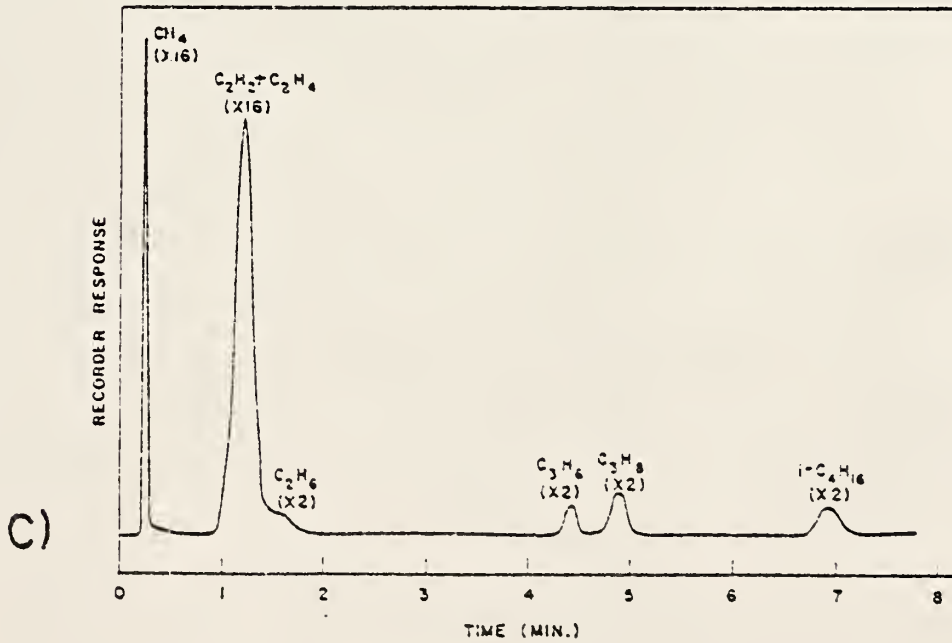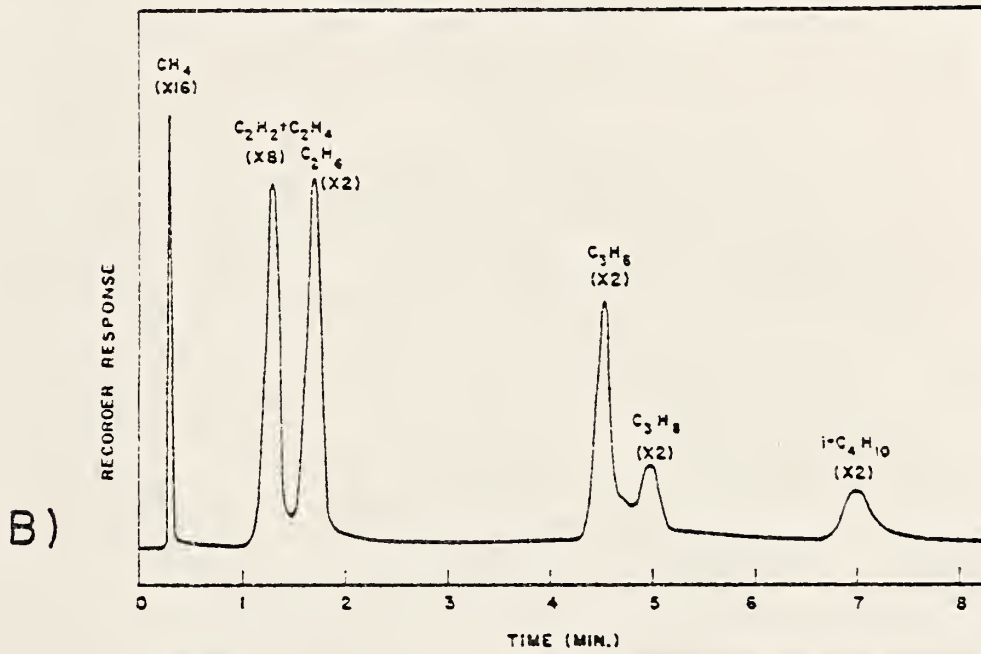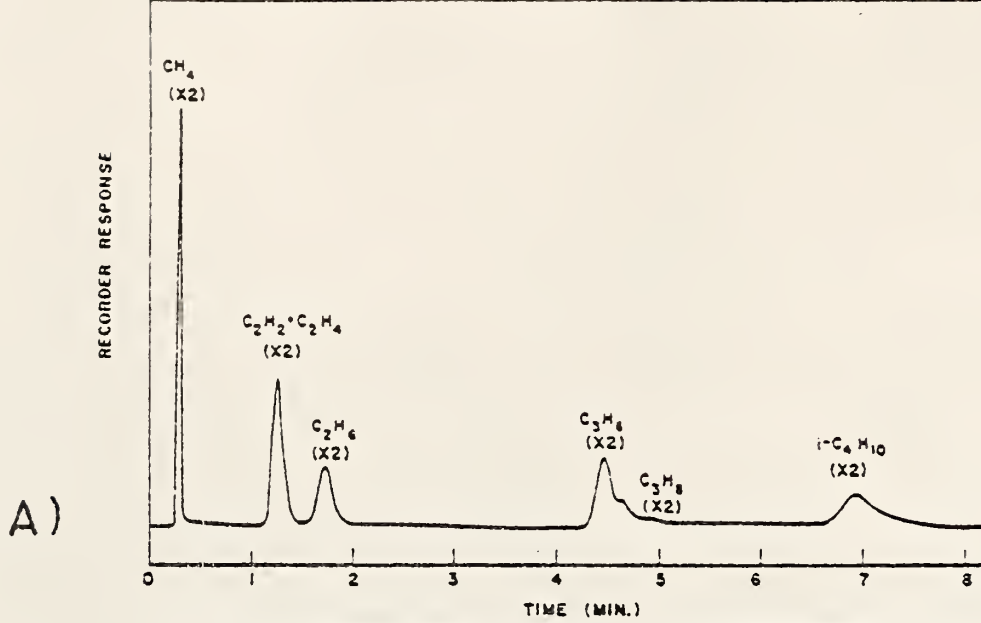
(C_2H_4). These two species could not, in fact, be separated by the gas chromatograph conditions used in these experiments. While the gas chromatograph could be used to separate these two gases without changing columns, excessive time is required and the column conditions are not suitable for the detection of C_3 and C_4 hydrocarbons. Since separation of these gases interferred with the identification of the higher hydro-carbons, ethyne/ethene separation was performed for one coal only. More-over, since the pyrolysis product distribution behaved similarly for the coals tested, it was *a priori* assumed that the ethyne/ethene separation results were similar to those expected for the other coals over the entire range of experimentation. Data from the C_2H_2/C_2H_4 separation experiments, runs 49-54, are graphically shown (as the ratio C_2H_2/C_2H_4) in Fig. 17. From this figure it is apparent that the second peak on the chromatogram, Fig. 16, is primarily C_2H_4 at 1200°K, an equimolar concentration of C_2H_4 and C_2H_2 at 1800°K, and primarily C_2H_2 at 2200°K.

From Fig. 16 it is also apparent that the relative contribution of methane (CH_4) increases dramatically with temperature from 1200-1500°K but decreases in concentration as the temperature increases from 1500-2100°K. The relative contribution of the C_2 unsaturates, ethyne and ethene increases throughout the temperature range, 1250-2100°K, while the contri-butions of the higher molecular weight hydrocarbons decrease monotonically. The contributions (in terms of the mass fraction of the original coal sample) of CH_4, C_2H_2, C_2H_4, and C_2H_6, over the temperature range studied are given in Fig. 18. Despite the apparent shift in temperature, the results compare favorably with those of Blair, et al. (22) shown in Fig. 6.
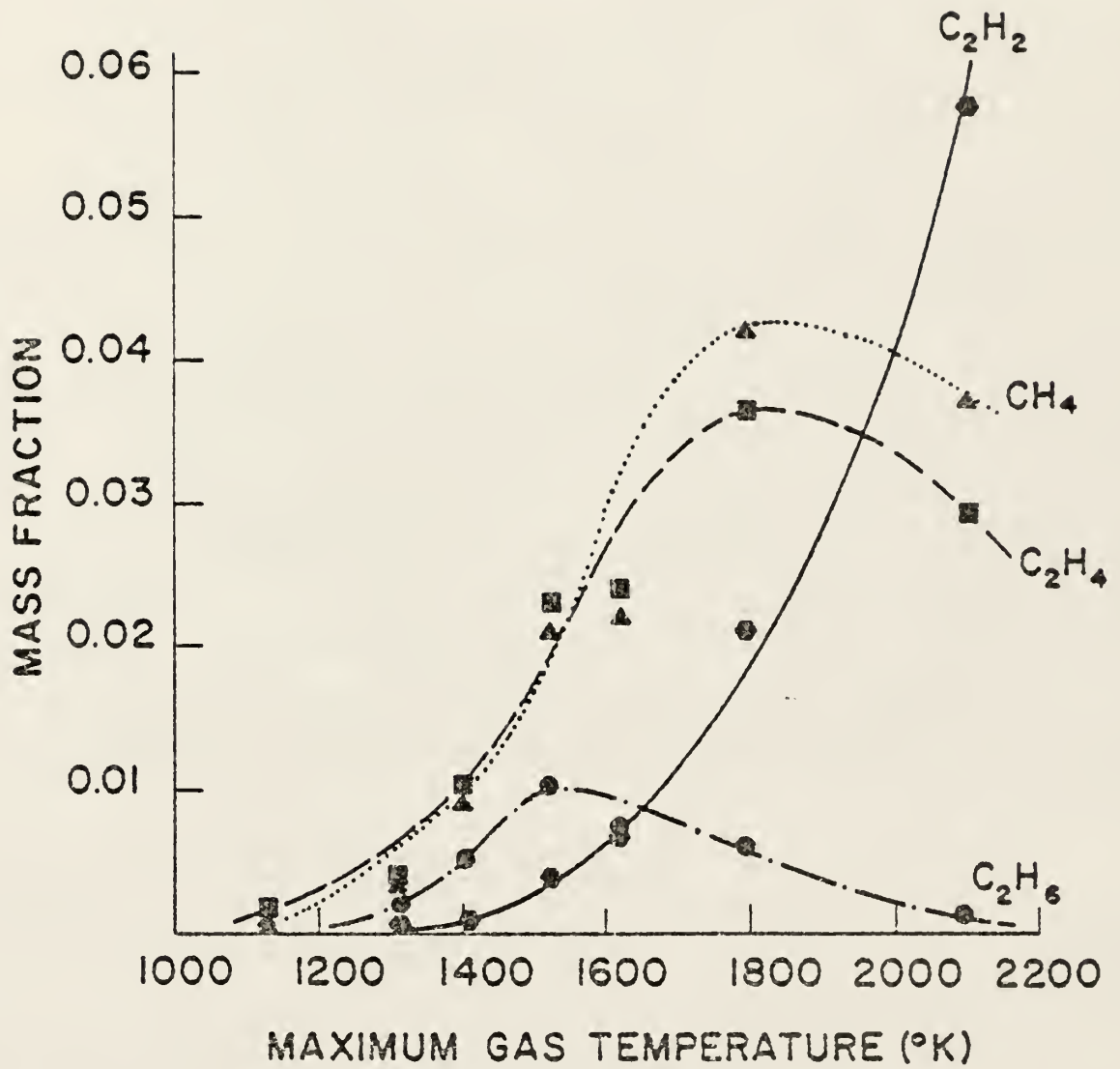
FIGURE 17

Ratio of the C_2H_2 to C_2H_4 contributions versus reflected shock temperature over the range of temperatures used in this study; coal-Pittsburgh Seam (large).
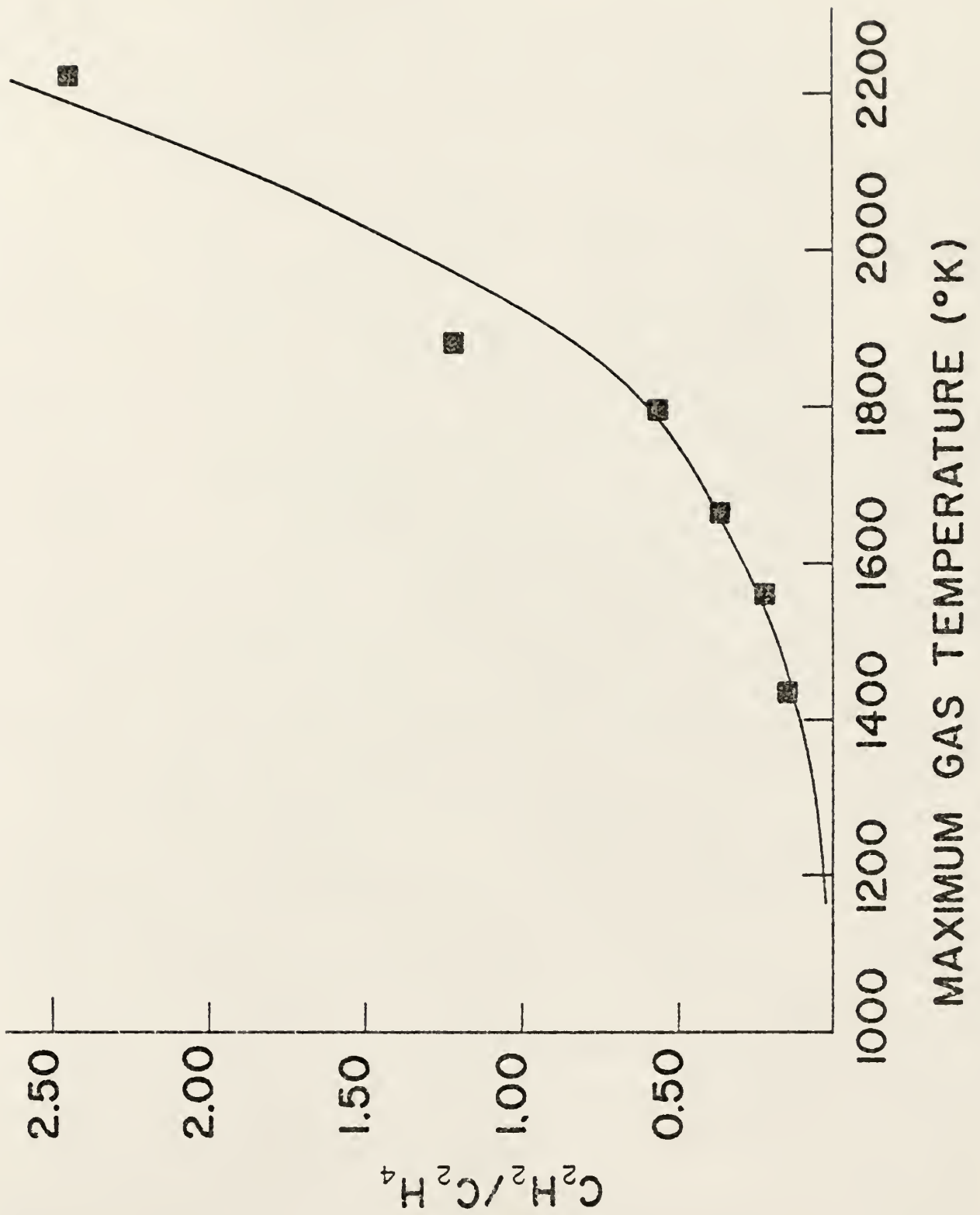
FIGURE 18

Major species detected as fractions of coal sample mass as a function of temperature; coal-Pittsburgh Seam (small).

A composite of the data from the three groups of pyrolysis runs, Tables 3, 4, and 6, is shown in Fig. 19. Hydrocarbon yields from the Illinois No. 6 coal were comparable to the Pittsburgh Seam coals at the lower temperatures but were substantially less at gas temperatures greater than 1600°K. A number of plausible explanations could account for these lower yields. For instance, the Illinois coal may have been more exposed, or "weathered", than were the Pittsburgh coals. (The reduction of hydrocarbon yields due to the weathering or slow pre-oxidation of a coal was discussed in detail by Howard (40)). This opinion is based partially on the results of a series of experiments conducted several months later. While little change in hydrocarbon yields were observed at the lower temperatures, substantial reductions (by nearly a factor of two) were observed for all the coals at temperatures greater than 1600°K. Consequently, greater care is being exercised in the storage of test samples.

The variation in the total hydrocarbon yield at lower temperatures (see Fig. 19) between the two sizes of Pittsburgh coal was verified with a separate series of pre-ignition oxidation experiments. Hypothesized reasons for the differential will be discussed in Section 3.2.

A comparison of the results of this study with the results of two earlier pyrolysis experiments performed in different apparatus is given in Fig. 20. Both the studies of Blair, et al.(22) and Suuberg, et al. (13) were captive in nature and run at lower heat up rates. The offset of the present results from the earlier experimentation is thought

FIGURE 19

C_1-C_4 hydrocarbon yields versus temperature for the three coals (Pittsburgh Seam-small, Pittsburgh Seam-large, and Illinois No. 6) in a nitrogen environment.
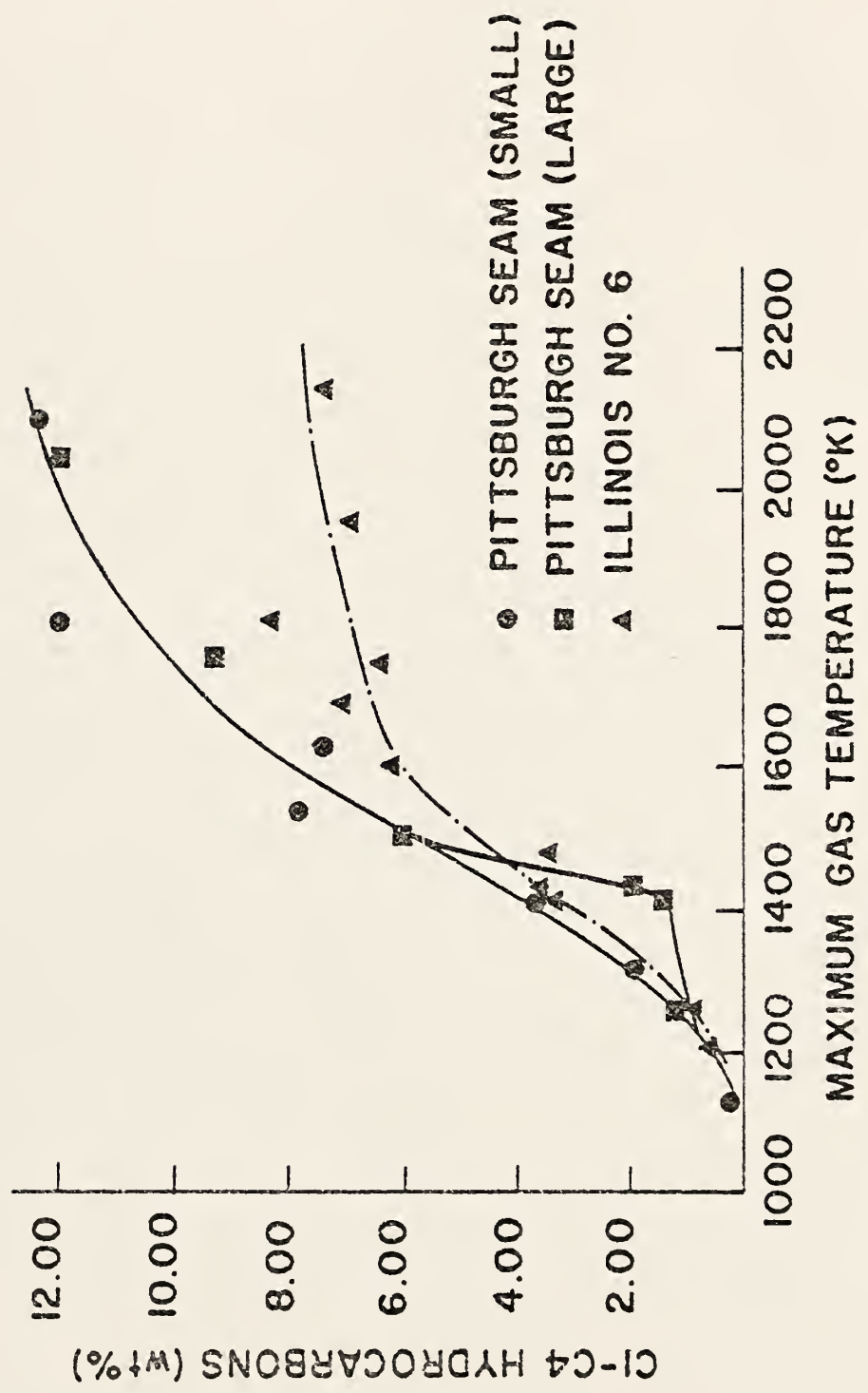
FIGURE 20

A comparison of the lower molecular weight hydrocarbon yields
(in pyrolyzing environments) versus temperature of this study with
the results of two earlier experimental investigations: Blair et al.
(22) and Suuberg et al. (13).
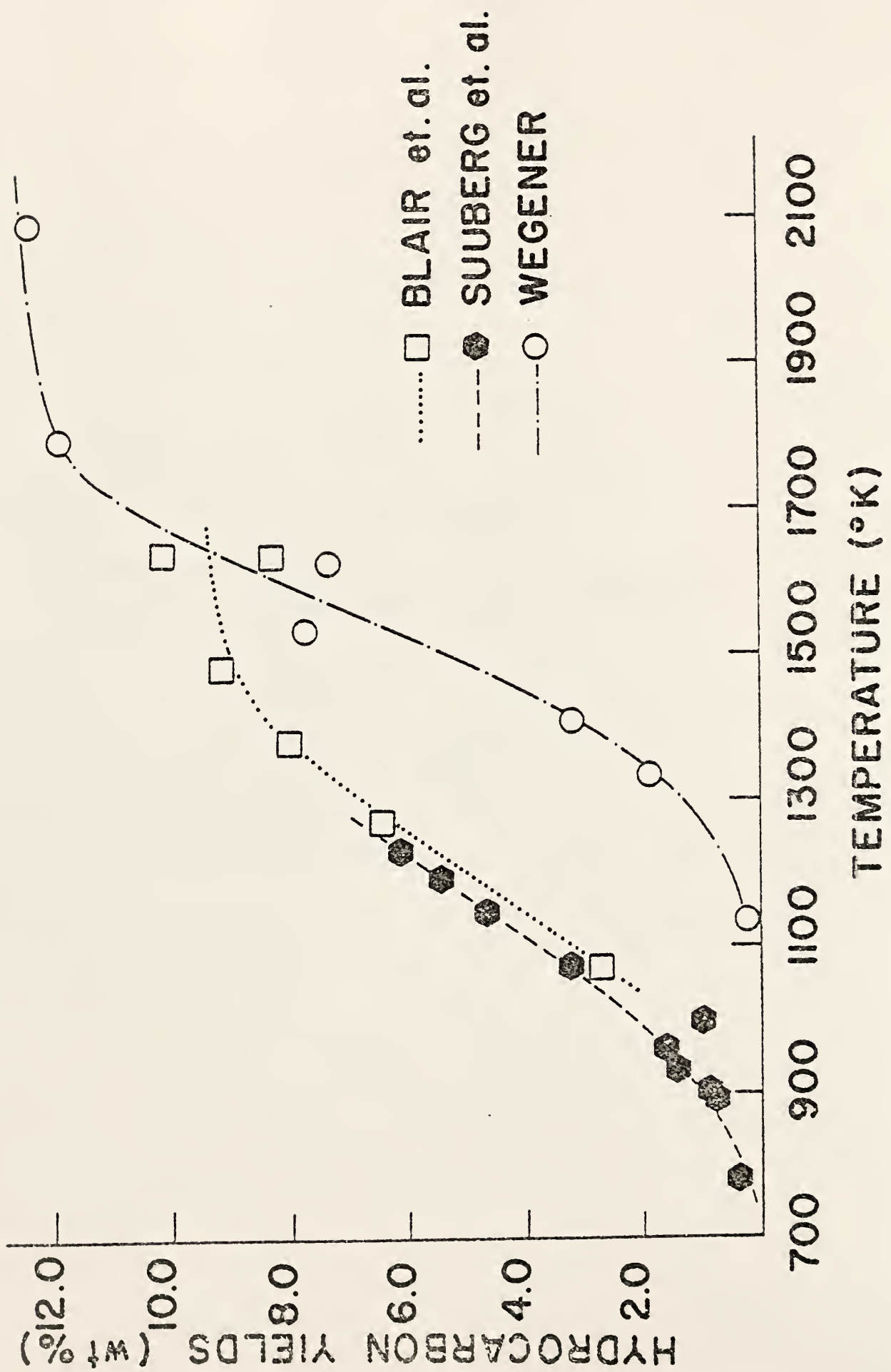
to be due to the higher heating rate used in the present study. It should be recalled from Section 1.2 that a shift of pyrolysis to higher temperatures has been predicted previously by Jüngten, et al. (6) and Gray, et al. (5). Nonetheless, the earlier experiments recorded the temperature of the retaining mechanisms, a platinum wire and a wire mesh, while the results of this work are plotted versus calculated gas temperatures.

The difficulty in assessing the true temperature of a suspension of polydisperse particles is obvious. The particles, varying from 1 to about 35 μm in diameter, would relax individually to the gas temperature at much different rates. For instance, from simple conduction heat transfer calculations based on the mass mean diameter, 13 μm, of the smaller Pittsburgh coal, it was estimated that the particle temperature may have been as much as 200°K less than the gas temperature at the hotter temperatures and 50°K lower at the cooler temperatures. This of course, would have shifted the pyrolysis results of this study towards the lower temperatures. However, from similar calculations on the larger Pittsburgh coal, mass mean diameter of 25μm, it was estimated that particle temperatures would have been from 400° to 700°K less than the gas temperature at the lower and upper limits of this study. Such a difference between the particle temperatures of the two Pittsburgh coals at a given gas temperature appears very unlikely, especially at the hotter gas temperatures where the hydrocarbon yields were nearly the same from the two coals. This similarity in hydro-

carbon yields indicates that the particle temperatures of the two
size distributions were similar at comparable gas temperatures. This
equilibration in temperature is believed to be the result of radiation
heat transfer from the smaller particles, which relax to the gas tempera-
ture very rapidly as compared to the larger particles.

The product gas distributions of the C_1 to C_4 hydrocarbons of this
study are similar to those determined by Woodburn, et al. (28). (See
Section 1.2 for further discussion of Woodburn, et al's. study). This
study was conducted over a lower temperature range in which only the
initial onset of C_2H_2 formation was observed. Bituminous coals were
used in both studies. The CH_4, C_2H_2, and C_2H_4 product gas distributions
of the previous study and of the small Pittsburgh coal of this study
are shown in Fig. 21. Only CH_4, C_2H_2, and C_2H_4 yields are represented
and, thus, deviation from 100% is due to the yields of higher hydro-
carbons.

In addition to the pyrolysis experiments, oxidation studies were
performed on the two Pittsburgh coals to study the devolatilization
behavior at temperatures about the observed ignition temperature, and
to determine what effect an oxidizing medium has on observed pyrolysis
products. The oxidation data, given previously in Tables 5 and 7, are
shown also in Figs. 22 and 23. Since a decrease in pyrolysis yield
is observed for the large coal with respect to the inert atmosphere,
oxidation of the evolved hydrocarbons apparently becomes substantial

FIGURE 21

A comparison of the major product distributions (CH_4, C_2H_2, and C_2H_4) on a percent weight basis versus temperature of this study with the study of Woodburn et al. (28).
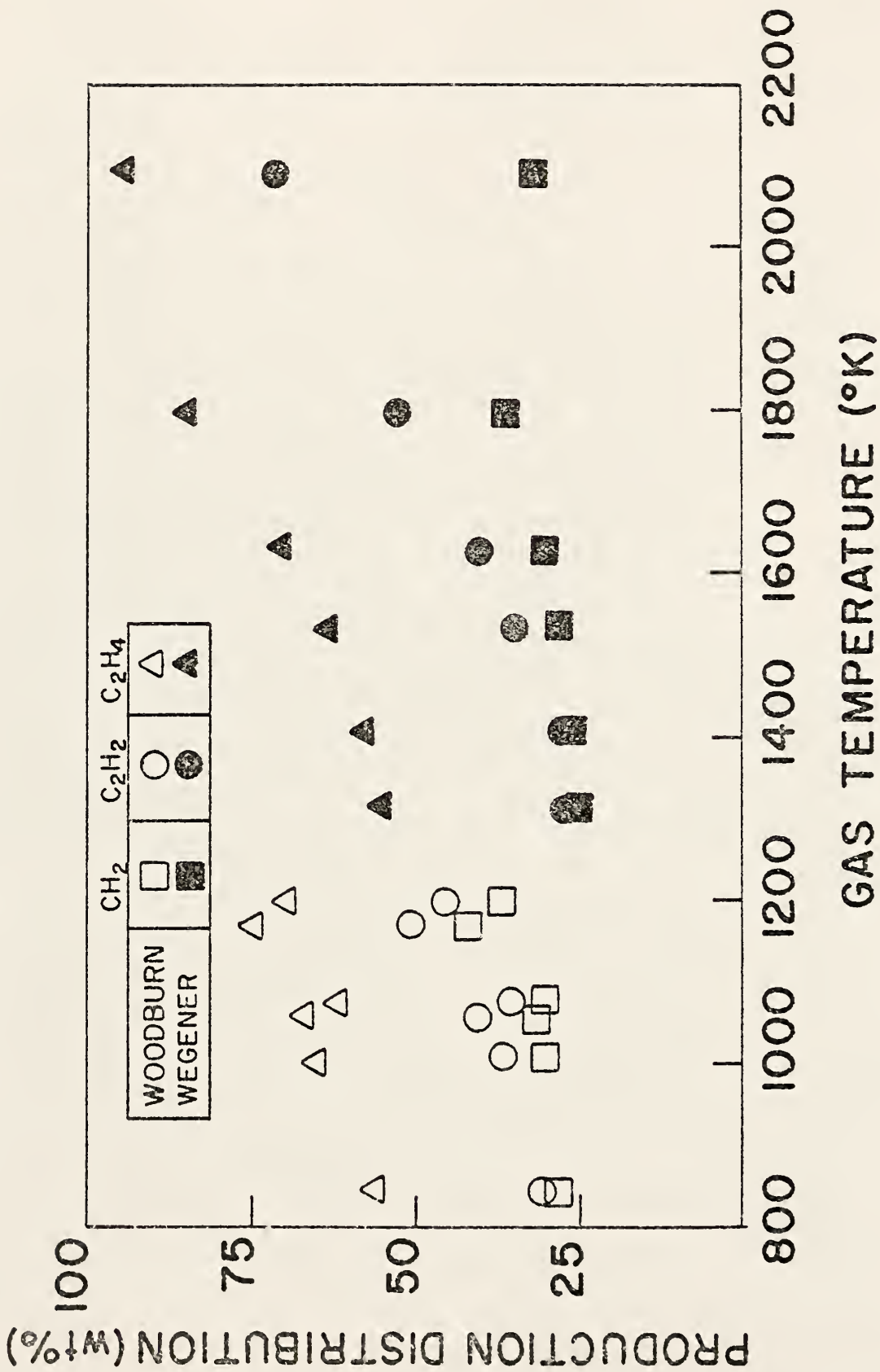
FIGURE 22

C_1-C_4 hydrocarbon yields versus temperature for the Pittsburgh
Seam (small) coal in both air and nitrogen environments.

PITTSBURGH SEAM (SMALL)
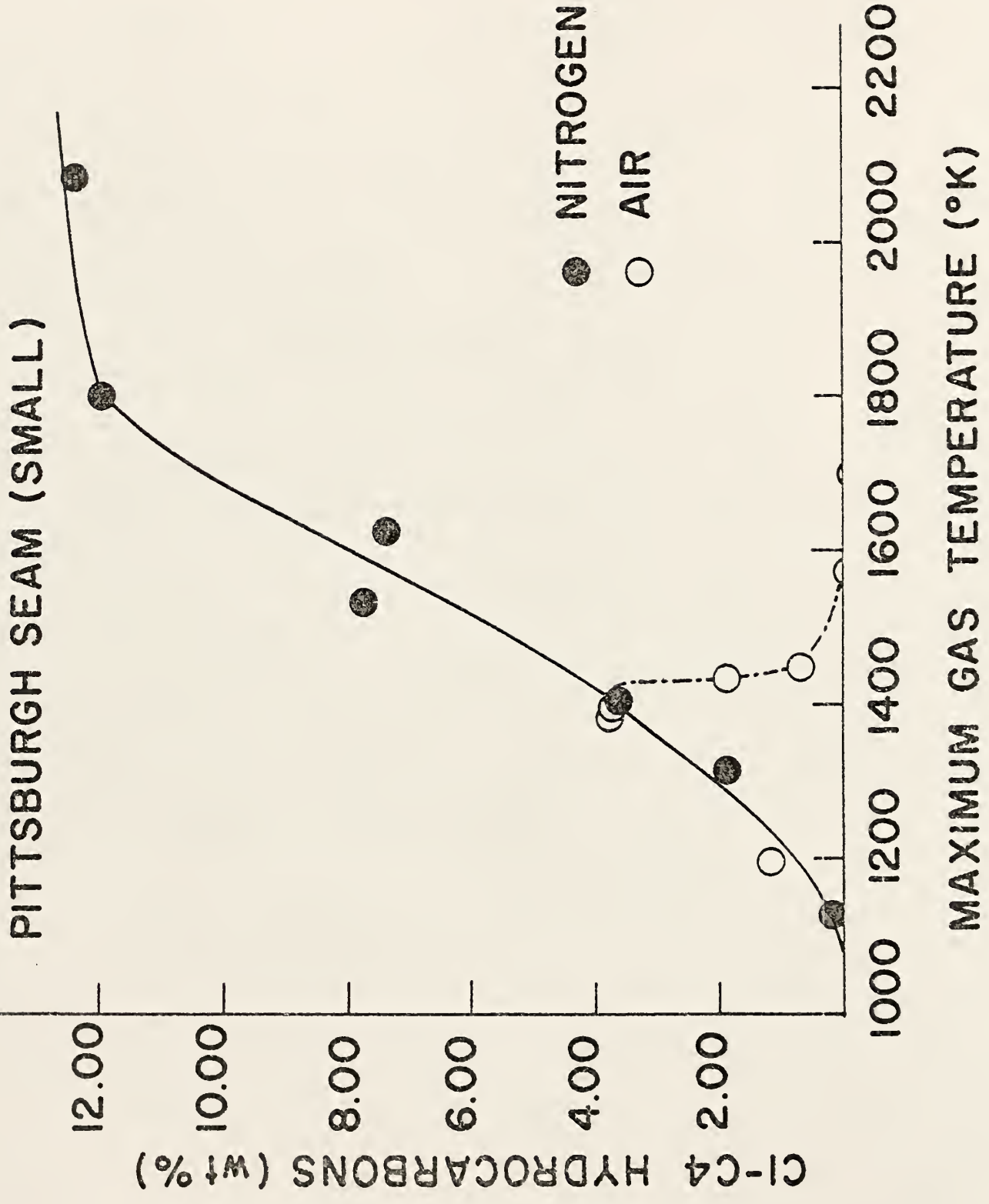
FIGURE 23

C_1-C_4 hydrocarbon yields as a function of temperature for the
Pittsburgh Seam (large) coal in both air and nitrogen environments.

PITTSBURGH SEAM (LARGE)

■ NITROGEN
□ AIR

C1-C4 HYDROCARBONS (wt%)

MAXIMUM GAS TEMPERATURE (°K)

between 1400-1500°K. The occurrence of particle ignition in this temperature range was indicated by the optical diagnostics. For instance, emission traces from oxidation runs at 1397°K, 1436°K, and 1453°K are shown in Fig. 24. A representative pressure t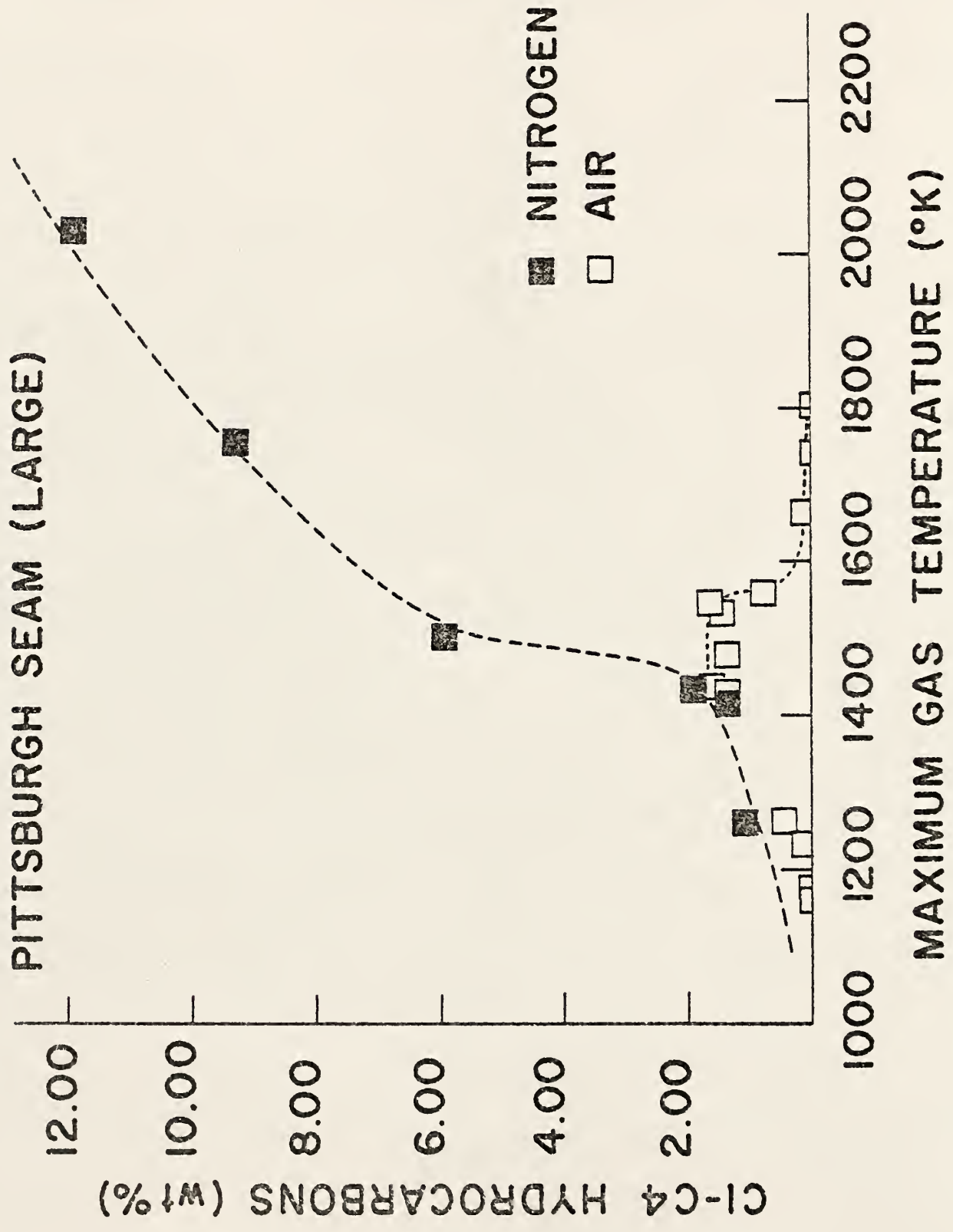race is given above the emission traces to serve as a reference frame. The correspondence of the particle ignition as indicated by the optical diagnostics and the sudden decrease in hydrocarbon gas yields is much better for the smaller coal samples than for the larger. While initial oxidation of the hydrocarbon gases did begin at approximately the same temperature for both samples, the observed particle ignition occurred approximately 100°K higher with the larger coal. The response of the hydrocarbon gas yields to temperature near ignition can be compared more easily on the expanded scale of Fig. 25.

While indirect measurements of pre-ignition devolatilization were reported in the numerous publications of Howard and Essenhigh (14, 15, 16, 17) this appears to be the first study in which pre-ignition volatiles have been directly measured. The interpretation of the data with respect to the coal structure and combustion mechanism is the topic of the following section.

3.2 Discussion of Results

The lower hydrocarbon yield data as listed in Figs. 22, 23, and 25 have been used in conjunction with information in the literature to postulate a mechanism of thermal decomposition of coal under rapid

FIGURE 24

The emission traces from oxidation runs (with the Pittsburgh

Seam-small coal) at 1397 °K, 1436 °K, and 1453 °K. At 1397 °K, no

departure of the hydrocarbon yield with the pyrolysis runs is

observed; there is also no evidence of ignition. At 1436 °K, the

hydrocarbon yield begins to depart (decrease) from the yields of

the pyrolysis runs and a slight emission is observed. At 1453 °K,

the hydrocarbon yield significantly departs from the yields of the

pyrolysis runs and emission is very apparent. Pressures were between
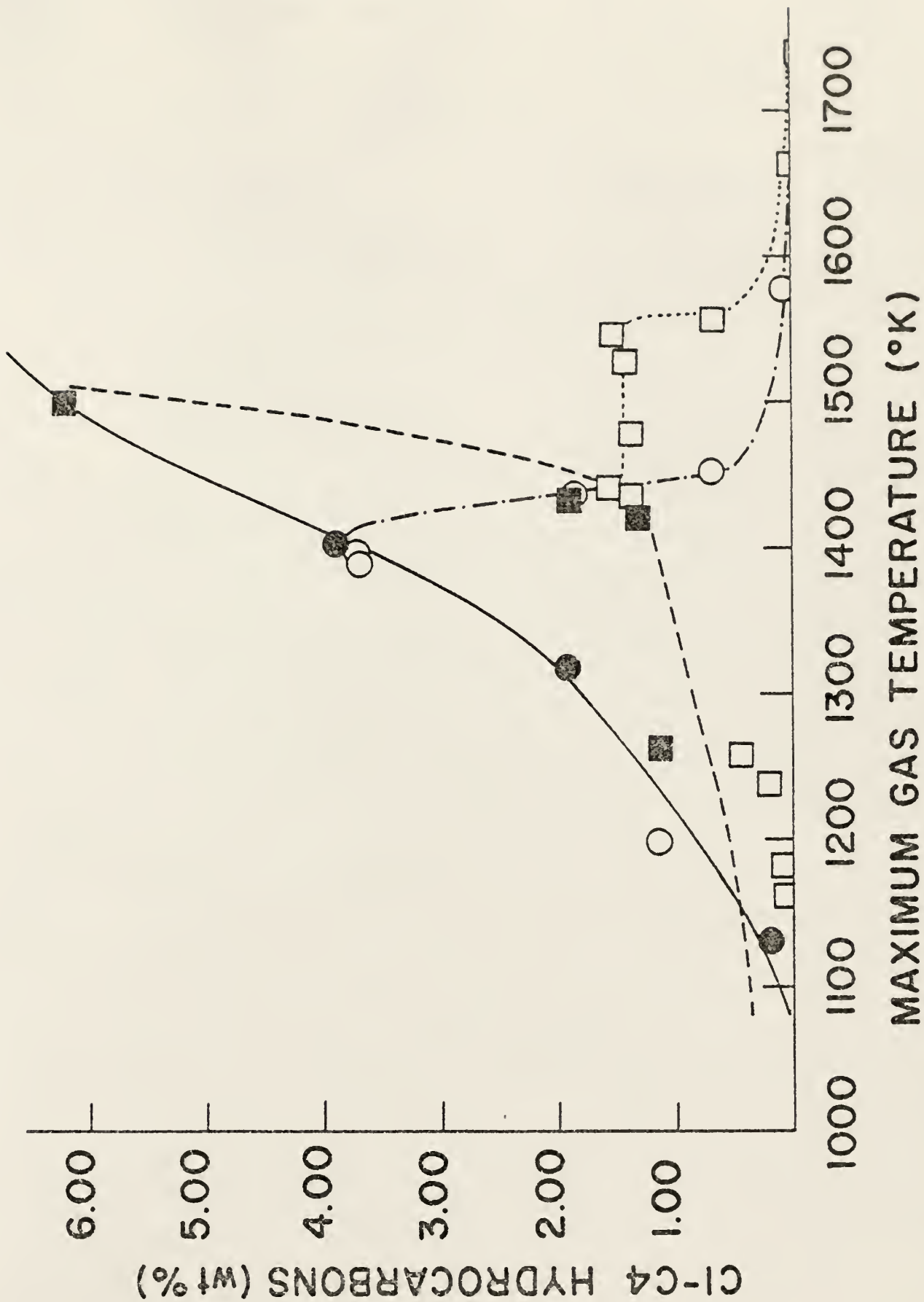
8.5 and 9.0 atm.

500 μsec/cm
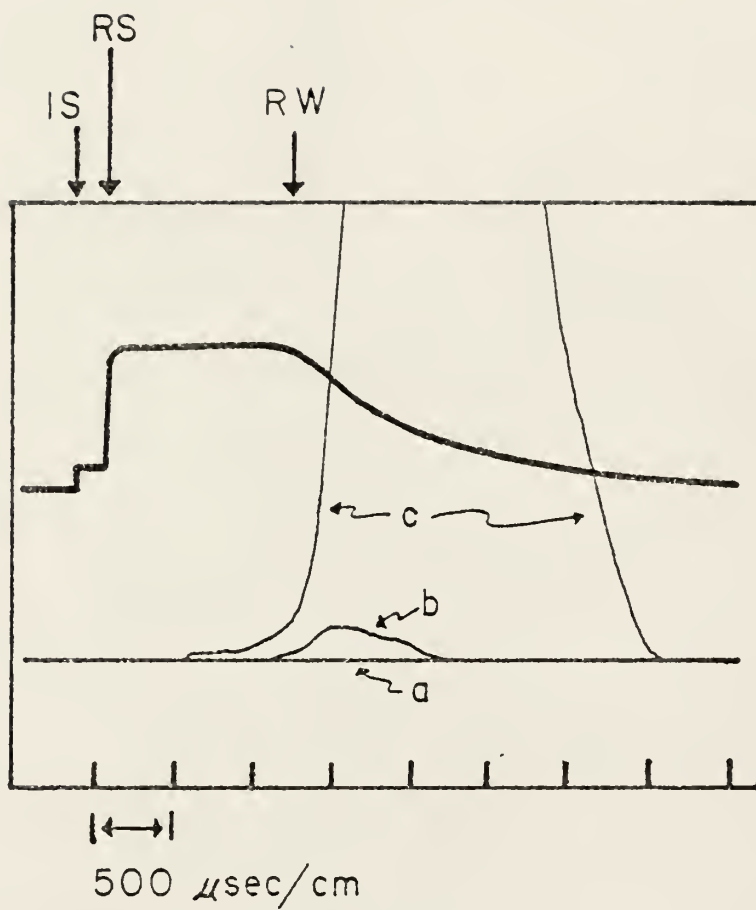
a = emission at 1397 °K

b = emission at 1436 °K

c = emission at 1453 °K

FIGURE 25

C_1-C_4 hydrocarbons in the temperature range characteristic of ignition.

heating conditions. A fundamental assumption in interpreting the
data is that the yields of lower hydrocarbons come from the parent
molecules, whether the coal or the evolved tar.

In summary, the following trends are apparent from the data. At
decomposition temperatures up to 1400°K, CH_4, C_2H_4, C_2H_6, C_3H_6, and
$i-C_4H_{10}$ are all present in the pyrolyzate at relatively the same
proportions. At decomposition temperatures between 1400-1600°K,
the yields of all the hydrocarbons increase. C_2H_6, C_3H_6, and $i-C_4-H_{10}$
reach their maximum yield and C_2H_2 and C_3H_8 appear in significant
quantities for the first time. From 1600 to 1900°K the yields of
C_2H_2 and C_2H_4 and CH_4 rapidly increase and become the dominant hydro-
carbon products. C_3H_8 attains its maximum value. At temperatures
greater than 1900°K, the yields of CH_4 and C_2H_4 tend to a plateau
level or decrease slightly. Higher order hydrocarbons experience a
larger relative decrease. C_2H_2 is present in greater concentration
than other hydrocarbons detected.

By assuming that a coal structure similar to that of Fig. 26 is
present in the parent coal, the preceding observations may be ex-
plained plausibly by the following argument. The low, yet diverse
hydrocarbon yields below 1400°K are the result of the initial C-C
bond cleavages in the parent molecules. The needed hydrogen atoms
may have come from the dehydrogenation of the non-aromatic rings
which also were the probable source of C_3H_6. Graham et al. (39)
speculate that dehydrogenation of the non-aromatic cyclics may be too

FIGURE 26

A representation of a bituminous coal molecule. (From (42))
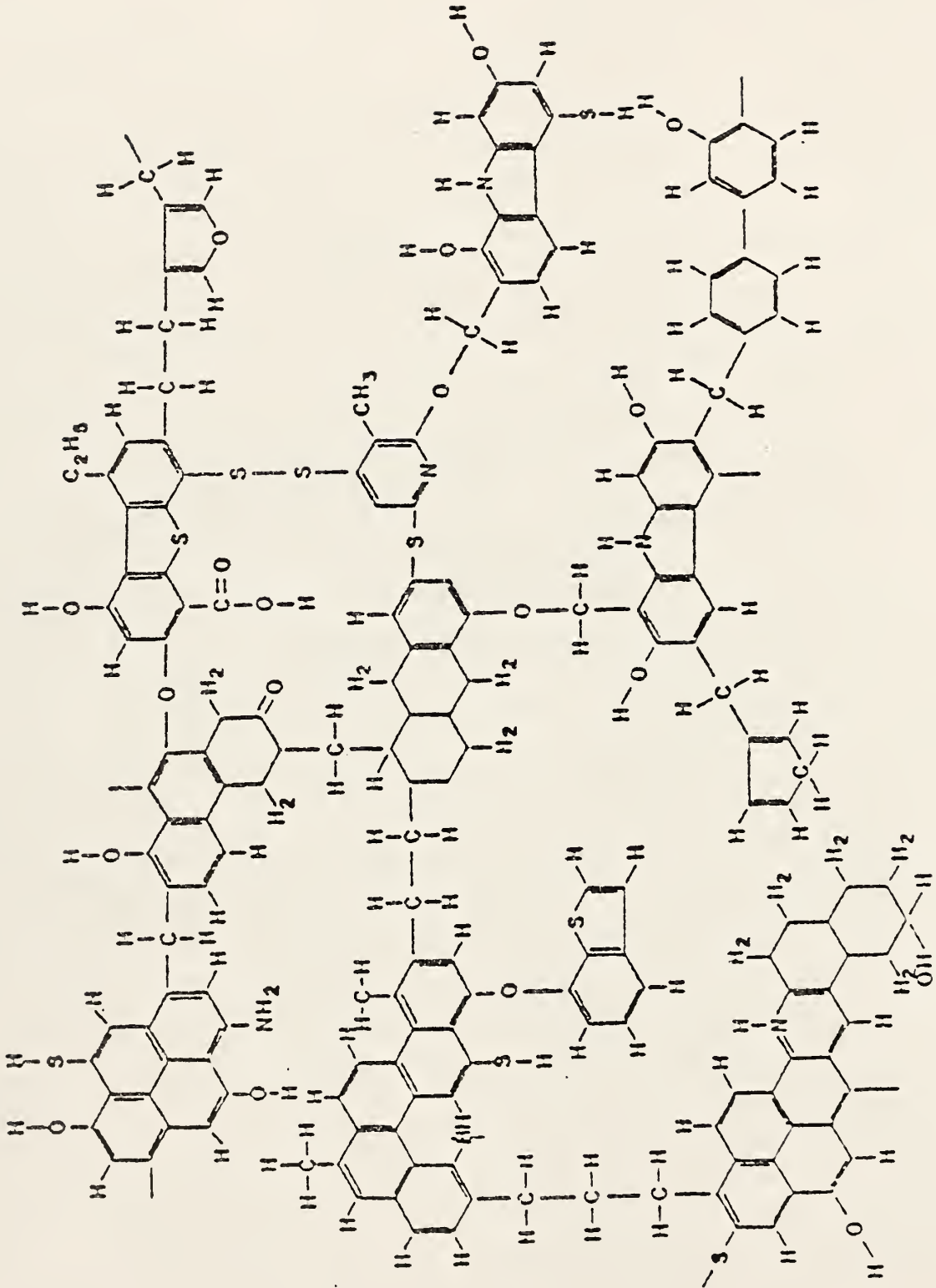
slow at these lower temperatures. The initial presence of $i-C_4H_{10}$ and absence of C_3H_8 may have been the result of limited hydrogen and abundant methyl radicals. The latter may have combined with C_3H_6 to form $i-C_4H_{10}$. The CH_4, C_2H_6, and C_2H_4 arise from combination of the CH_3 and CH_2 radicals with H atoms. The increase in hydrocarbon yields occurring between 1400-1600°K is the result of additional C-C bond cleavage. A slight increase in the dehydrogenation reaction may have accounted for the onset of C_3H_8 formation. The initial observance of C_2H_2 may indicate the limited occurrence of fragmentation reactions in the aromatic rings. The increase in CH_4 and C_2H_4, and the increase in C_2H_2 from 1600 to 1900°K results from additional C-C bond cleavage and fragmentation reactions respectively. The additional, and now more likely, dehydrogenation reactions resulted in the maximum yields of C_3H_8. At temperatures greater than 1900°K maximum C-C bond cleavage appears to occur. Yields of the higher order hydrocarbons diminished as their C-C bonds also appear to have cleaved. While dehydrogenation reactions may have slightly increased, the C-C bond cleavage appears to have resulted in a hydrogen deficient environment since the yields of CH_4 and C_2H_4 diminished. This lack of hydrogen atoms and the fragmentation reactions at these high temperatures resulted in C_2H_2 becoming the dominant hydrocarbon gas produced.

Parts of this mechanistic interpretation were first hypothesized by Graham, et al. (39) who studied the formation of soot by the shock

heating of aromatic hydrocarbons. In that study, no direct evidence of fragmentation and dehydrogenation reactions was collected; however, the yields of soot observed optically were in conformance with the postulated mechanism.

It is not yet known whether low order hydrocarbons primarily evolve directly from the parent coal molecules or from large tar molecules which come off as primary fragments and have almost the same molecular structure as the coal. When developing the above hypothesis it was assumed that both may occur since initial cleavages of C-C bonds can take place at many locations in the parent coal molecules. These initial cleavages can result in hydrocarbons containing from one to several hundred carbon atoms.

The hydrocarbon yields from the oxidation and the pyrolysis runs of both the small and large Pittsburgh coals may be used to generalize about the role of volatiles in coal ignition. The yields of the lower order hydrocarbons are shown over the temperature range close to ignition in Fig. 25. It should be remarked that, as with any particle system the small and large Pittsburgh coals had size distributions that complicate the evaluation of the data. Therefore, it is difficult to correlate the pyrolysis or combustion behavior in terms of particle size.

From a quick assessment of the data of Fig. 25, two major differences in the devolatilization behavior of the two sizes of Pittsburgh coal are apparent. First, while the smaller coals devolatilization increased in a continuous manner with temperature, the larger coal's devolatilization exhibited a sharp increase in the temperature range common to

ignition. In Chapter 2, it was predicted that significant differences in the overall suspension temperatures probably would not exist because of radiative coupling among the particles. It may be that the differences exhibited in the devolatilization behavior of the large coal are due to mass transport effects. Devolatilization has been shown to some certainty by Howard and Essenhigh (15) to be a volumetric process. Pore diffusion and structure changes of the coal would be expected to have more influence in a larger coal. Insofar as the chemical structures are the same, chemical kinetics cannot be invoked to explain the observed differences. Second, the two coals exhibited distinctly different devolatilization behavior in the temperature region typical of observed particle ignition. In the temperature range below ignition, devolatilization yields of hydrocarbons in oxidation experiments compared favorably with those of pyrolysis runs of comparable temperature. This appears to be the first confirmation that oxidation environments have little effect on the devolatilization kinetics. The ignition of the smaller coal, as discussed in Section 3.1, was reasonably well defined by both the diminishing hydrocarbon yields and the rapid increase of emission at approximately 1400°K. The ignition delays at temperatures between 1400-1450°K approached 1.5 msec, which was the longest observation time. Ignition may still occur at lower temperatures if the reaction time is sufficiently long; however, based on the previously discussed assumption that the temperature of the particle cloud closely follows the gas temperature, the reduction in the ignition temperature under the present circumstances would probably be small.

Ignition of the larger particles (as is apparent from Fig. 25) was less obvious from the hydrocarbon yields than it was with the smaller particles. While the emission traces for the larger coal were not recorded, they were available from the surface oxidation studies of Seeker (35). Similar to the smaller coal, the optically observed ignition again corresponded to the onset of rapidly diminishing hydrocarbon yields which, for the larger coal, was at approximately 1560°K. However, unlike the smaller coal, the hydrocarbon yields from the oxidation runs of the larger coal were observed to be below the yields from the pyrolysis runs at a temperature which is more than 100°K lower than the optically observed ignition temperature.

While further analysis may prove otherwise, the data do not appear to contain sufficient information to conclusively determine if ignition is a homogeneous or heterogeneous process. Unfortunately, the data can be used to imply the occurrence of either ignition process for both size distributions of the Pittsburgh seam coal. The correspondence of the dramatic decline in hydrocarbon yield with the onset of significant emission for both size distributions may indicate that a heterogeneous ignition process is occurring. However, the mere presence of pre-ignition volatile yields are not insignificant since they could result in total heat releases of 500 and 800 cal/gm of coal for the small and large Pittsburgh coals, respectively.

Regardless of which ignition mechanism is present, the data do provide some interesting clues about the combustion behavior following

ignition. Combustion of the small Pittsburgh coal appears to be a heterogeneous combustion process. No significant departure of volatile yields in the oxidation runs vis-a-vis pyrolysis runs takes place until ignition is optically observed; at which point hydrocarbon yields from the oxidation runs rapidly decay to zero with increasing temperature.

The combustion behavior of the large Pittsburgh coal appears to be more involved. Certainly, the oxidation of volatiles occurs before significant emission is observed. However, is a true homogeneous combustion occurring or is the process a slow oxidation of hydrocarbons prior to ignition? What is the reason for the constant hydrocarbon yields between 1440°K and 1560°K? With the data currently available, there are undoubtedly a number of plausible explanations. As one alternative, this author suggests the following.

Possibly a volatile flux from the particle may be the controlling mechanism. For this to take place ignition of the larger coal must occur at approximately 1440°K, where the oxidation hydrocarbon yields first depart from those in pyrolysis. If ignition occurs at 1440°K, then only 10% of the total volatile yield has been released. Furthermore, if devolatilization is a volumetric process (15) in which the devolatilization time is independent of particle size (below 100 μm), the volatile flux at the surface of a large particle must be greater than the volatile flux at the surface of a small particle. Therefore, energy from the exothermic reactions immediately elevates the particle temperature which results in further devolatilization. The surface flux associated with

this devolatilization process may be of sufficient magnitude to lift the flame front off the particle surface. This would result in the coal particles being surrounded by a thin shell of volatiles between the particle surface and the flame front. The reflected rarefaction wave arrives before the post-ignition devolatilization begins to subside and quenches the lifted flame.

Therefore, is it possible that the hydrocarbons detected from post-shock gas analyses of the oxidation runs between 1440°K and 1560°K are those hydrocarbons which are between the flame front and the particle surface when the flame is extinguished? While it may intuitively seem that this volume would be orders of magnitude too small to contain this quantity of hydrocarbons (approximately 1.2 wt% of the coal sample), calculations indicate otherwise.

The distance from the center of the particle to the spherical flame can be approximated by:

$$r_f = \frac{\phi_f \ a^2 \ RTK}{L \ P \ D}$$

where

ϕ_v = volatile flux [$\frac{moles}{cm^2 \ sec}$],

a = particle radius [cm],

R = ideal gas constant [atm cm^3/moles°K],

T = temperature [°K],

K = sum of the number of moles of oxygen required to burn one mole of volatiles and the number of moles of products produced per mole of volatiles burned,

L = a dimensionless number determined from K and the partial pressure of oxygen,

P = pressure [atm],

D = diffusion coefficient [cm^2/sec].

From Fig. 23, it is apparent that, at 1440°K, over 90% of the devolatilization is yet to occur. In other words, only 10% (by weight) of the volatiles have evolved. Based on this knowledge, assuming that devolatilization occurs rapidly (in approximately 100 μsec), assuming the volatiles can be approximated by C_2H_4, using a particle radius of 12.5 μm (the mass mean radius), using a temperature and pressure corrected diffusion coefficient of .33 cm^2/sec, and using a temperature and pressure of 1500°K and 8 atm respectively, the value of r_f was calculated to be 39.2 μm. This means that the flame would be 26.7 μm off the particle surface. By further considering the volume between the flame front and particle surface, the density therein, and the number of particles present (based on mass mean diameter and the weight of the coal sample used), the percent weight of the coal sample (in volatile form) which could be contained in the concentric volume was calculated. Surprisingly, using the above values, it was determined that 3.78% wt. of the original coal sample could be contained in the volume; a value even greater than that observed experimentally. Obviously, there is a large degree of uncertainty in assessing the value of the volatile flux and this could more than account for the excessive prediction.

In addition to those volatiles contained between the particle surface and the flame front, there is most likely another source of the detected hydro-

carbons. The reflected rarefaction undoubtedly extinguishs the flame and cools the gas much quicker than it cools the particles. Therefore, it is likely that some devolatilization occurs after the flame is quenched. Unfortunately it is difficult to estimate the magnitude of such a contribution.

The decline in hydrocarbon yields at 1560°K can also be explained by a flame lift-off hypothesis. As the shock temperatures become higher, an increasingly greater percentage of the volatiles evolve before ignition. Consequently, post-ignition devolatilization becomes increasingly shorter in duration. At temperatures above 1560°K the post-ignition devolatilization is probably of too short a duration to hold the flame off the particle surface until the rarefaction arrives. Therefore, the flame front moves back onto the particle surface where heterogeneous combustion proceeds. (The "moving back" of the flame front to the particle surface at higher temperatures is enhanced by the diffusion coefficient with increases with temperature to approximately the 1.75 power). It is this heterogeneous combustion behavior which is believed to be observed on the emission traces.

The above hypotheses are based on the first phase of a comprehensive study; therefore, they represent viable possibilities worthy of further consideration.

4. CONCLUSIONS AND RECOMMENDATIONS FOR FURTHER STUDY

Devolatilization of coal under heating rates and temperatures characteristic of pulverized fuel combustion has been studied with the use of a single pulse shock tube. The yields of the lower molecular weight hydrocarbons from the pyrolysis runs of this study compare favorably with those of earlier studies on both an individual and a total basis. This reproducibility confirms the validity of the gas sampling procedure and analysis developed in this investigation.

Application of the same gas sampling techniques to the oxidation runs resulted in the first reported direct measurement of significant pre-ignition volatiles. The role played by the volatiles during ignition, however, has not been established, and whether ignition is a homogeneous or heterogeneous process cannot be concluded definitely.

Particle size was observed to have a small influence on the hydro-carbon yields of the pyrolysis runs. The effect of particle size is more pronounced on the yields from the oxidation runs. It was concluded, by comparison of the hydrocarbon yields from the pyrolysis and oxidation runs, that the smaller sized coal, mass mean diameter of 13 μm, burns heterogeneously. With the larger sized coal particles, mass mean dia-meter of 25 μm, there appeared to be a competition between the hetero-geneous and homogeneous modes of combustion.

Even though the single pulse shock tube has been shown to be a use-ful instrument in the study of coal devolatilization and ignition, the

acquisition of more sophisticated peripheral diagnostic equipment is needed. Specifically, it is recommended that this work be repeated when a mass spectrometer is acquired to determine a more complete spectrum of volatile yields up to mass numbers of 300. It is suggested that the ignition delays of a volatile mixture, whose composition and concentration is similar to those observed just prior to ignition of the coal, should be studied. From this it may be possible to infer whether ignition is occurring homogeneously. It may be necessary to include inert particles to better simulate the coal particle cloud.

More work with the temporal shocks is also needed. Inasmuch as significant difficulty in controlling the reaction times was encountered in this work, better experimental procedures need to be developed.

REFERENCES

1. Babcock and Wilcox, Steam/Its Generation and Use, (Babcock and Wilcox, New York, 1972), 38th ed., Chap. 9, p. 9-1.

2. D. B. Anthony and J. B. Howard, AIChE Journal, 22, 625 (1976).

3. S. K. Ubhayakar, Lecture Notes prepared for the Short Course of Coal Characteristics and Coal Utilization at Pennsylvania State University (Avco Everett Research Laboratory, Inc.), 1977.

4. H. C. Wiser, G. R. Hill, and N. J. Kertamus: Ind. Eng. Chem. Process Design and Devel., 6, 133 (1967).

5. D. Gray, J. B. Cogoli and R. H. Essenghigh, Progress in Chemistry, 131, 72 (1974).

6. V. H. Jüngten and K. H. van Heek, Fuel, 47, 103 (1968).

7. V. H. Jüngten, Erdöl Und Kohle, 17, 180-186 (1962).

8. K. H. van Heek, H. Jüntgen, and W. Peters, Deutsche Bunsegesellschaft für Phyikalishe Chemie, 71, 113-121 (1967).

9. H. L. Feldkirchner and J. L. Johnson, Rev. Sci. Instr., 39, 1227 (1968).

10. M. Mentser, H. J. O'Donnel, S. Ergun, and R. A. Friedel, Advances in Chemistry, Series No. 131, Am. Chem. Soc. (1974).

11. D. B. Anthony, J. B. Howard, H. C. Hottel, and H. P. Meissner, Fifteenth Symposium (International) on Combustion. p. 1303, The Combustion Institute (1975).

12. D. B. Anthony, J. B. Howard, H. C. Hottel, and H. P. Meissner, Fuel, 55, 121 (1976).

13. E. M. Suuberg, W. A. Peters, and J. B. Howard, <u>Seventeenth (International) Symposium on Combustion</u>, The Combustion Institute (1978).

14. J. B. Howard and R. H. Essenhigh, Combustion Flame, <u>9</u>, 337 (1965).

15. J. B. Howard and R. H. Essenhigh, Combustion Flame, <u>10</u>, 92 (1966).

16. J. B. Howard and R. H. Essenhigh, <u>Eleventh Symposium (International) on Combustion</u>, p. 399, The Combustion Institute (1967).

17. J. B. Howard and R. H. Essenhigh, Ind. Eng. Chem. Process Design and Devel., <u>6</u>, 74 (1967).

18. G. M. Kimber and M. D. Gray, Combustion Flame, <u>11</u>, 360 (1967).

19. S. Badzoich and P. G. W. Hawksley, Ind. Eng. Chem. Process Design and Devel., <u>9</u>, 521 (1970).

20. H. Kobayashi, J. B. Howard, and A. F. Sarofin, <u>Sixteenth Symposium (International) on Combustion</u>, p. 411, The Combustion Institute (1977).

21. S. K. Ubhayakar, D. B. Stickler, C. W. Von Rosenberg, Jr., R. E. Gannon, <u>Sixteenth Symposium (International) on Combustion</u>, p. 427, The Combustion Institute (1977).

22. D. W. Blair, J. O. L. Wendt, and W. Bartok, <u>Sixteenth Symposium (International) on Combustion</u>, p. 475, The Combustion Institute (1977).

23. R. H. Essenhigh, <u>Sixteenth Symposium (International) on Combustion</u>, p. 353, The Combustion Institute (1977).

24. P. M. Goldberg and R. H. Essenhigh, _Seventeenth Symposium (International) on Combustion_, The Combustion Institute (1978).

25. M. A. Nettleton and R. Stirling, Proc. Roy. Soc. A300 62 (1967).

26. M. A. Nettleton and R. Stirling, Proc. Roy. Soc. A322 207 (1971).

27. M. A. Nettleton and R. Stirling, Combustion Flame, 22, 407 (1974).

28. E. T. Woodburn, R. C. Everson, and A. R. M. Kirk, Fuel, 53, 38 (1974).

29. A. I. Lowenstein and C. W. von Rosenberg, Jr., _Modern Developments in Shock Tube Research_, Shock Tube Research Society (1977).

30. W. R. Seeker, The Design Assembly, and Testing of a Shock Tube for Study of Coal Combustion Kinetics, Master's Thesis, Kansas State University (1977).

31. H. S. Glick, W. Squire, and A. Hertzberg, _Fifth (International) Symposium on Combustion_, The Combustion Institute, 393 (1955).

32. A. G. Gaydon and I. R. Hurle, _The Shock Tube in High-Temperature Chemical Physics_, Reinhold (1963).

33. S. L. Soo, Am. Inst. Chem. Engrs. J., 1, 384 (1961).

34. J. R. Kliegel, _Ninth Symposium (International) on Combustion_, The Combustion Institute (1963).

35. W. R. Seeker, The Kinetics of Ignition and Particle Burnout of Coal Dust Suspensions Under Rapid Heating Conditions, Ph.D. Dissertation, Kansas State University (1978).

36. W. R. Seeker, D. C. Wegener, T. W. Lester, and J. F. Merklin, _Seventeenth (International) Symposium on Combustion_, The Combustion Institute (1978).

37. C. Park and J. P. Appleton, Combustion Flame, 20, 369 (1973).

38. H. S. Glick, Sixth (International) Symposium on Combustion, The Combustion Institute, 98 (1957).

39. S. C. Graham, J. B. Homer, and J. L. J. Rosenfeld, Proc. Roy. Soc. (London) A344, 259 (1975).

40. H. C. Howard, Chemistry of Coal Utilization (Wiley and Sons, New York, 1963) Supplementary Vol., p. 340.

41. J. B. Howard, Mechanisms of Ignition and Combustion in Flames of Pulverized Bituminous Coal, Ph.D. Dissertation, Pennsylvania State University (1965).

ACKNOWLEDGEMENTS

The author wishes to express his sincere gratitude to
Dr. Thomas W. Lester, his major professor, for his guidance and
support throughout this investigation. Dr. Lester has the rare
ability to demand the respect of his students while being their
friend, which makes for a very conducive learning environment.

Grateful recognition is expressed to Dr. J. F. Merklin with
whom this author had frequent discussions. Dr. Merklin's expertise
in the field of chemistry was called upon throughout the study.

The author is also indebted to co-worker W. R. Seeker. The
discussions with and the suggestions of Mr. Seeker, Ph.D. Candidate, were invaluable.

The technical assistance of Bill Starr with the gas chromatographic equipment was indispensible and sincerely appreciated.

APPENDIX A

Examination of the Devolatilization Equation of Jüngten and van Heek (6)

Jüngten and van Heek (6) logarithmically reduced the following equation,

$$\frac{dV}{dT} = \frac{K_o V}{m} \exp \left\{ - \frac{E}{RT} - \frac{K_o R}{mE} \ T^2 \exp \left(- \frac{E}{RT} \right) \right\}$$ (A1)

by making the following substitutions,

$$y = \ln \frac{dV}{dT} \ , \quad a_o = \ln \frac{K_o V_o}{mE} \ ,$$

$$a_1 = - \frac{E}{R} \ , \quad a_2 = - \frac{K_o R}{mE} \ ,$$ (A2)

$$x_1 = \frac{1}{T} \ , \quad x_2 = \frac{1}{T^2} \ ,$$

to obtain an equation suitable for regression analysis of the form,

$$y = a_0 + a_1 x_1 + a_2 x_2 \ \exp(a_1 x_1) \ .$$ (A3)

Equation (A1) was first derived in an earlier publication by Jüngten (7) and later logarithmically reduced for regression analysis by van Heek et al. (8).

When checking the above logarithimic reduction, an error was found which may significantly alter a large portion of Jüngten and van Heek's results that have been repeatedly cited over the past decade.

A correct logarithmic reduction of the differential equation
yields:

$$y = a_0 + a_1 \frac{1}{T} + a_2 \ T^2 \ \exp(a_1 \frac{1}{T}) \ . \tag{44}$$

It can be seen readily that the above substitution for x_2 can
no longer be made. While a regression analysis can still be applied
to equation (A5), equivalent answers will not be obtained.

The surprising success which Jüngten and van Heek had in using
their reduced equation to model the devolatilization behaviors of a
number of species (including coal) is questionable indeed. What this
may imply is that the actual kinetics are amenable to a variety of models.
Unfortunately, the authors have not included sufficient data to allow
a replication of their modeling. It is recommended that data from later
studies be modeled by the correct expression, Eq. (A4) to ascertain
whether the error has been carried through the literature.

Appendix B

Experimental Procedure

The procedure employed to obtain gas samples for post-shock analysis is summarized in the following checklist.

_____ 1) Remove test section end wall, quartz windows, and dispersion plate and holder.

_____ 2) Clean these parts and the inside of the test section between the second thin film gauge and the end wall with paper towels and acetone.

_____ 3) Blow out test section with compressed air.

_____ 4) Replace parts (except for the dispersion plate).

_____ 5) Insert a 10 mil mylar diaphragm into position.

_____ 6) Open vacuum pumps and evacuate both sections of the tube.

_____ 7) While the tube is being evacuated,

a) Remove, clean, and replace filter of the gas sampling system,

b) connect the sample bottle and evacuate the gas sampling system,

c) weigh the coal sample on the dispersion plate.

_____ 8) When the test section is evacuated to less than 10^{-3} torr, close valves to vacuum pumps of both sections of the shock tube.

_____ 9) Fill driven section to 40 torr with zero air.

_____ 10) Close the valve to the sub-atmospheric gauge of the test section.

_____ 11) Fill the driver section to 220 psig with helium.

_____ 12) Burst the diaphragm (this shock is used to clean the tube) and vent the tube.

_____13) Remove ruptured diaphragm and insert the appropriate mylar diaphragm combination into position.*

_____14) Place the coal sample into the shock tube.

_____15) Repeat step #6.

_____16) Align the optics while the tube is being evacuated.

_____17) Repeat step #8.

_____18) Fill the driven section to the appropriate pressure with the desired test gas.

_____19) Repeat step #10.

_____20) Fill the driver section to the appropriate pressure with helium.

_____21) Turn off overhead lights, vacuum pumps, and all other unrequired electronic equipment which may interfere with the instrumentation.

_____22) When the gas sampling system is evacuated to less than 10^{-3} torr, close the valve to vacuum pump and turn pump off.

_____23) Position the oscilloscope traces (pressure, emission, and absorption) on the screen and place the scope in single sweep mode.

_____24) Reset the time interval counter and oscilloscope.

_____25) Open the camera shutter.

_____26) Rupture diaphragm.

_____27) Immediately open the valve to the gas sampling system and fill the gas bottle to a positive gage pressure.

_____28) When a positive gage pressure is attained, close the valve on the sample bottle and vent the tube.

_____29) Close camera shutter.

*The variable length end wall of the driver section will have to be adjusted for the temporal runs.

Appendix C

Error Analysis

Because of the many uncertainties associated with research on
a system in which heat and mass transfer and chemical kinetics are
concurrently involved, a concise statement of the error associated
with combustion measurements is seldom made. Although shock tube
research minimizes some errors, others are introduced. For instance,
the error associated with calculating the reaction zone temperature from
the frozen gas equations has been discussed by Nettleton (25) who pre-
dicted errors of up to 50°K and by Gaydon and Hurle (32) who report un-
certainties of ± 25°K to be common for shock tube experimentation. An
additional error in calculating the gas temperature can be associated
with the particles suspended in the test gas. By using the analysis of
Soo (33) and Kliegel (34) the deviation in the reflected shock temperature
was found to be less than 50°K.

Uncertainty in the hydrocarbon gas yield had several sources. For
instance, uncertainty in the mass of the initial coal sample, a very low
but still significant background of hydrocarbons in the shock tube, in-
accuracies in the sample dilution multiplication factor, and the error in
determining the integrated area under the hydrocarbon peaks all contribute
to the error. The error in the initial mass of coal was insignificant,
between 0.25--1.0%. The hydrocarbon background was maintained at a mini-
mum and fairly constant level by firing an oxidation shock prior to

every devolatilization run. The background levels were negligible at
all but the lowest temperatures where the hydrocarbon yields from
pyrolysis approached zero. When preceded by an oxidation run, back-
ground levels were less than 10 ppm. This level approaches the lowest
background attainable with the test gases used (99.9998-99.9995% purity).
However, if an oxidation run was not performed, background levels up to
80 ppm were measured. The relative error in the cutting out and weighing
of the gas chromatograph peaks was, of course, directly related to
peak size. The error in all instances was less than 5%. By far, the
greatest error in the hydrocarbon yields was associated with determining
the sample dilution multiplication factor (SDMF) at high temperatures
(>1600°K) where mixing between driver and test gas was extensive. Below
1600°K the error in determining the SDMF was generally less than 2%. At
the high temperatures, however, errors in the SDMF of 10-15% were known
to exist. An error could also be associated with the calibration of the
gas chromatograph. This, however, would have been a systematic error,
constant for all runs, and would not have changed the conclusions of the
study.

Therefore, while errors in hydrocarbon yields may have been greater
than 10% at the lowest and highest temperature regions; the error was
much less in the regions between 1300°K and 1600°K, which was of prime
concern in this study. The data recorded in this temperature range were
remarkably reproducible. In replication runs, data agreed to within $\pm$ 5%.

THE PRODUCTION OF LOWER MOLECULAR WEIGHT HYDROCARBONS DURING THE
THERMAL DECOMPOSITION OF PULVERIZED COAL IN AIR AND NITROGEN

by

DENNIS CHARLES WEGENER

B.S., Kansas State University, 1975

———————————

AN ABSTRACT OF A MASTER'S THESIS

submitted in partial fulfillment of the

of the requirements for the degree

MASTER OF SCIENCE

Department of Nuclear Engineering

KANSAS STATE UNIVERSITY
Manhattan, Kansas

1978

ABSTRACT

The production of lower hydrocarbons during the thermal decomposition of pulverized coal in air and nitrogen was experimentally investigated in a single pulse shock tube. The coal particles were subjected to elevated temperatures for well defined reaction times at known thermodynamic conditions. Significant pre-ignition devolatilization was observed for the first time under rapid heating rates comparable to pulverized fuel firing. The hydrocarbon profiles of the pyrolysis runs were analyzed and a general devolatilization mechanism was developed.

Two size distributions of a Pittsburgh seam coal (mass mean diameter of 13 and 25 μm) were used to determine the influence of particle size on the ignition mechanism. The smaller coal was observed to devolatilize in a more continuous manner with temperature than the larger coal, but general trends of the hydrocarbon yields were similar. A much more dramatic influence of particle size was observed in the oxidation runs. The volatile yields from the oxidation experiments while there was no observable difference in the yields for the smaller coal prior to ignition; therefore, it was concluded that the smaller coal burned heterogeneously while combustion of the larger coal was more complex. One plausible mechanism consistent with the data is that the larger size fraction burns in a multi-stage process in which the flame is first lifted off the particle surface as the hydrocarbons escape and then attached to the surface for particle burnout.